Manifestations of nonstatistical effects in nuclei

I. N. Izosimov
V. G. Khlopin Radium Institute, St. Petersburg

Fiz. Élem. Chastits At. Yadra **30**, 321–379 (March–April 1999)

The experimental and theoretical data giving evidence of nonstatistical effects in the excitation and decay of highly excited nuclear states and resonances of compound nuclei are reviewed. Nonstatistical effects manifested in β decay, delayed processes, and nuclear reactions involving low-energy protons are analyzed. The reasons for the appearance of nonstatistical effects are discussed. © *1999 American Institute of Physics.* [S1063-7796(99)00202-8]

INTRODUCTION

Studies of the decays and structure of intermediate and heavy nuclei at excitation energies above 2–3 MeV are important for our understanding of the nucleus. As the excitation energy increases, the nuclear level density grows rapidly and the wave functions of nuclear states acquire a quite complicated structure, since even a small residual interaction can lead to the mixing of closely spaced states. Therefore, as a rule, it is assumed that the structure of these states is very complicated, and the coefficients of the decomposition of the wave function into the simplest configurations obey statistical laws. The characteristics of various nuclear processes are rather simple to calculate in this statistical model. In particular, the transition-width distribution is described by the Porter–Thomas equation,[1] the strength function of β transitions $S_\beta(E)$ depends smoothly on energy,[2] there are no correlations between different partial widths,[3] and the ratios of the amplitudes for decay via various spin channels follow the Cauchy distribution.[4]

Nonstatistical effects are closely related to the symmetry of the nuclear interaction.[5] Some of the first and most clearly manifested nonstatistical effects in decays of highly excited nuclear levels were observed for isobar-analog resonances, owing to the isospin symmetry of the nuclear forces.[6] In fact, the isospin of an isobar-analog resonance (analog) is one unit larger than that of the nearby levels, which prevents the mixing of the analog with levels of complex structure. At nuclear excitation energies above 2–3 MeV a large number of other (nonanalog) states and resonances are observed. They have two possible interpretations: statistical or nonstatistical. In the first case it is assumed that they are statistical states, while in the second it is assumed that they are structures like the giant resonance, related to a distribution of simple excitations [for example, proton (π)–particle (p) [(πp)] and neutron (n)–hole (h) [(nh)], coupled to give angular momentum 1^+: $[\pi p \otimes nh]_{1+}$] in the levels of the compound nucleus. In the second case the physical interpretation of the experiments must differ from that of the statistical approach.

For example, if nuclear forces were spin- and isospin-invariant [i.e., if the spin–isospin group $SU(4)$ were the symmetry group], we should observe nonstatistical effects for a number of nonanalog resonances and states. However, since the nuclear interaction is observed to depend quite strongly on spin, so that[7,8] $SU(4)$ can be only an approximate symmetry, nonstatistical effects associated with spin–isospin $SU(4)$ symmetry will be less clearly expressed than isobar-analog resonances [the isospin $SU(2)$ symmetry of the strong interaction]. The question therefore arises of isolating and observing nonstatistical effects in the excitation and decay of nuclear states and resonances, determining the degree of mixing of a simple component with the levels of the compound nucleus, and interpreting the structure of the states at the microscopic level.

In the statistical model the wave function $\Psi_{\rm St}$ is written as

$$\Psi_{\rm St}=\sum_k^n C_k\cdot\varphi_k, \quad \sum_k^n |C_k|^2=1, \tag{1}$$

where φ_k are the wave functions of the "simple" configurations, and C_k are random numbers $n\gg 1$. In the nonstatistical approach it is usual to isolate a particular configuration φ_0 in the wave function $\Psi_{\rm NSt}$:[9]

$$\Psi_{\rm NSt}=C_0\cdot\varphi_0+\sum_k^n C_k\cdot\varphi_k, \quad |C_0|\geqslant|C_k|,$$

$$|C_0|^2+\sum_k^n |C_k|^2=1. \tag{2}$$

Deviations from the statistical theory have been discovered[4,5,9–15] in $(p,p'\gamma)$ and (p,γ) reactions, β^- and β^+ (EC) decays, and delayed processes unrelated to the excitation or decay of isobar-analog states.

In this review we discuss the recently discovered nonstatistical effects in β^- and β^+ (EC) decays, delayed processes, and nuclear reactions. The new nonstatistical effects which have been found experimentally are related to elementary nuclear-excitation modes of the type $[\pi p\otimes nh]_{1+}$ and $[np\otimes\pi h]_1^+$.

1. THE MANIFESTATION OF NONSTATISTICAL EFFECTS IN BETA DECAY

1.1. The strength functions of beta transitions

The β-transition strength function $S_\beta(E)$ is one of the most important characteristics of the nucleus.[5,14] It is the distribution of the squared moduli of the β-decay matrix

elements in the nuclear excitation energies E. For excitation energies E up to Q_β, the total β-decay energy, $S_\beta(E)$ determines the nature of the β decay and the half-life $T_{1/2}$ of a radioactive nucleus via the β-decay channel. At large excitation energies not reachable in β-decay, $S_\beta(E)$ determines the cross sections of various nuclear reactions depending on the β-decay matrix elements.

The strength function $S_\beta(E)$ determines the distribution, in the nuclear energy E, of elementary excitations and combinations of them of the type proton–particle (πp) and neutron hole (νh), coupled to give angular momentum J^π: $[\pi p \otimes \nu h]_{J^\pi}$, and neutron–particle ($\nu p$) and proton hole ($\pi h$), coupled to give angular momentum J^π: $[\nu p \otimes \pi h]_{J^\pi}$. The strength function of Gamow–Teller β transitions describes excitations $[\pi p \otimes \nu h]_{1^+}$ or $[\nu p \otimes \pi h]_{1^+}$.

In β decay, $S_\beta(E)$ is related to the probability density for populating levels of the daughter nucleus $I(E)$:

$$S_\beta(E) = \frac{I(E)}{T_{1/2} \cdot f(Q_\beta - E)}, \tag{3}$$

where $f(Q_\beta - E)$ is the Fermi function[16] and $(Q_\beta - E)$ is the β-transition energy.

For processes depending on Gamov–Teller-type matrix elements,

$$S_\beta(E) = \frac{1}{D \cdot (g_V^2 / g_A^2)} B'(\mathrm{GT}, E), \tag{4}$$

where $D = 2\pi^3 \hbar^7 \ln 2 / g_V^2 m_e^5 c^4$, $D = (6260 \pm 60)$ sec, g_V and g_a are the vector and axial-vector β-decay constants,[1,6]

$$B'_{\mp}(\mathrm{GT}, E) = \frac{1}{2I_i + 1} \left| \langle I_f | \sum_k t_{\mp}(k) \sigma_\mu(k) | I_i \rangle \right|^2, \tag{5}$$

$$B'_{\mp}(\mathrm{GT}, E) = \frac{4\pi}{g_a^2} B_{\mp}(\mathrm{GT}, E), \tag{6}$$

where I_i and I_f are the spins of the initial and final states and $t_\pm$ and σ_μ are the isospin and spin operators.[5] The distribution $B'(\mathrm{GT}, E)$ calculated in a given model can be used to find $S_\beta(E)$ and $T_{1/2}$:

$$\frac{1}{T_{1/2}} = \int_0^{Q_\beta} S_\beta(E) \cdot f(Q_\beta - E) dE. \tag{7}$$

1.2. The statistical and nonstatistical approaches to analyzing the strength functions of beta transitions

Until recently, the statistical picture of the beta strength functions dominated.[2] In beta decay, fairly simple configurations are populated in the daughter nucleus. At excitation energies in the daughter nucleus of several MeV, simple states can mix strongly with states of more complicated structure. If this mixing is large, $S_\beta(E)$ can be described by the statistical model. According to the latter, the β-decay strength function is a smooth function of the excitation energy. As a rule, $S_\beta = \mathrm{const}$ or $S_\beta(E) \sim \rho(E)$ is used in statistical calculations, where $\rho(E)$ is the level density of the daughter nucleus.

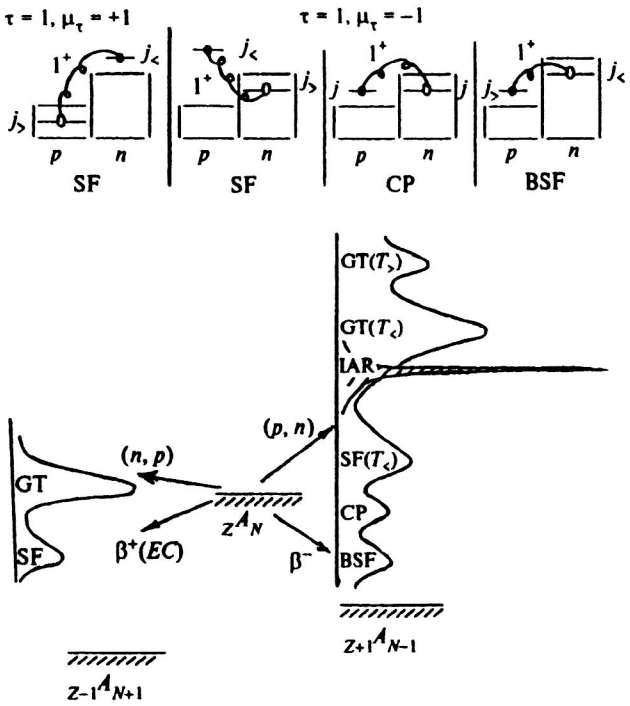

FIG. 1. Scheme of the strength functions of Fermi β transitions (shaded region) and Gamow–Teller β transitions. The strength function of Fermi β transitions is concentrated at the isobar-analog resonance (IAR). The components of the Gamow–Teller resonance with different isospins [GT($T_<$) and GT($T_>$)] and the configurations forming the strength function of Gamow–Teller β transitions are indicated. BSF is a backward spin-flip configuration, CP is a core-polarization configuration, SF is a spin-flip configuration, ● denotes a particle, and ○ denotes a hole. Isovector excitations are characterized by isospin τ and isospin projection μ_τ.

Experimental data later appeared which indicated that $S_\beta(E)$ for allowed β transitions depends strongly on energy. The strong delay of Gamow–Teller β transitions to low-lying excited nuclear states led to the idea of a giant Gamow–Teller resonance,[17,18] located near the corresponding analog resonance. At energies below this giant resonance there is an extended "train" whose energy structure is particularly noteworthy (Fig. 1). It has been shown that anti-analog states play the main role in forming the resonance structure of the train of the Gamow–Teller resonance for nuclei of the s–d shells.[19] States of the core-polarization type dominate for nuclei of the $f_{7/2}$ shell (Fig. 1).[20] Experimental information about these states has been obtained by studying the $M1\,\gamma$ decay of analog resonances.[21] In studies of $S_\beta(E)$ in ^{236,238}Pa nuclei, it has been shown that states of the "backward spin-flip" type play an important role in the description of β decay for a number of heavy nuclei[5,14] (Fig. 1).

Data on the Gamov–Teller resonance have been obtained by studying direct (p,n) reactions.[22,23] The interpretation of the peaks in the neutron spectra from direct (p,n) reactions based on the nonstatistical approach to describing charge-exchange excitations has made it possible to correctly describe the experimental data on the locations and intensities of the peaks in the neutron spectra.[5,24,25]

High-resolution study of the delayed-neutron spectra[26] has shown that a small number of daughter-nucleus levels

are selectively populated in β decay, i.e., $S_\beta(E)$ has a resonance, nonstatistical nature.

Direct measurements of the level-population probabilities in β decay by the γ-ray total-absorption method[27,28] have revealed the presence of energy structure in $S_\beta(E)$.

The data cited above indicate that $S_\beta(E)$ depends nonmonotonically (nonstatistically) on the nuclear excitation energy E.

From the viewpoint of the nonstatistical approach, the structure of $S_\beta(E)$ is determined by the isovector parts of the effective nucleon–nucleon interaction, and also by the mixing of "simple" excitations with states of more complicated structure.

A representation[29] of the elementary nuclear-excitation modes is useful for analyzing the resonance structure of $S_\beta(E)$. The charge-exchange elementary excitations producing the structure of $S_\beta(E)$ form a special class of elementary modes (Fig. 1). They are characterized by isospin $\tau=1$ and isospin projection $\mu_\tau=\pm 1$. In other words, these elementary excitations occur not in the nuclei where the ground (parent) state is located, but in neighboring (daughter) nuclei. The ordinary elementary excitations ($\mu_\tau=0$), for example, low-lying phonon states or multipole giant resonances, are located in the same nucleus as the ground state.

From the viewpoint of the microscopic approach to the formation of collective states, charge-exchange resonances are a superposition of particle–hole excitations of various types, for example, proton–particle and neutron hole. The Gamow–Teller resonance is a coherent superposition of configurations of the proton–particle and neutron-hole type, coupled to give angular momentum 1^+.

The scheme of states important for analyzing the strength functions of Gamow–Teller transitions is shown in Fig. 1. The parent state (for simplicity, an even–even nucleus with $N>Z$) has isospin T_0 and isospin projection $T_z=T_0$. A family of particle–hole charge-exchange excitations of the $[\pi p\otimes\nu h]_J$ type is located in the adjacent nucleus, whose ground state has isospin $T=T_0-1$ and isospin projection $T_z=T_0-1$. These are excitations with $\tau=1$ and $\mu_\tau=-1$. States with the structure $[\nu p\otimes\pi h]_J$ are located in the other adjacent nucleus. This nucleus has ground-state isospin $T=T_0+1$ and $T_z=T_0+1$, and elementary excitation characterized by $\tau=1$ and $\mu_\tau=+1$. Excitations with $\tau=0,1$ and $\mu_\tau=0$ occur in the parent nucleus.

For β transitions of the Fermi type, in the simple model of Ref. 6 there is only a single state carrying the entire transition strength. This is the IAS analog state with spin 0^+, isospin $T=T_0$, and $T_z=T_0-1$, formed as a coherent superposition of $[\pi p\otimes\nu h]_{0^+}$ configurations. A typical strength function for Fermi β transitions is also shown in Fig. 1.

The situation regarding Gamow–Teller β^- transitions is more complicated. The principal β-transition strength is carried by the Gamow–Teller resonance with $J^\pi=1^+$, $T=T_0-1$, and $T_z=T_0-1$ ($\tau=1$, $\mu_\tau=-1$). This state is formed as a coherent superposition of all possible $[\pi p\otimes\nu h]_{1^+}$ configurations. It has a significant contribution from configurations of the spin-flip type, i.e., $[\pi p\otimes\nu h]_{1^+}$, $j_p=l-\frac{1}{2}$, $j_n=l+\frac{1}{2}$ and is located near the analog resonance. States of the core-polarization type are located at lower energies: $[\pi p\otimes\nu h]_{1^+}$, $j_p=j_n$. At even lower energies there are states of the backward spin-flip type: $[\pi p\otimes\nu h]_{1^+}$, $j_p=l+\frac{1}{2}$, $j_n=l-\frac{1}{2}$. The isospin of states of the core-polarization and backward spin-flip types has the normal value, i.e., $T=T_0-1$ and $T_z=T_0-1$. Since a configuration of the spin-flip type does not possess definite isospin, there is a $T_>$ ($T=T_0$, $T_z=T_0-1$) component of the Gamow–Teller resonance located above the principal ($T_<$) resonance.[5,24] For β^+ (EC) decay there is[5] only one value of the isospin for $[\nu p\otimes\pi h]_{1^+}$ configurations. The most strongly collectivized state with $J=1^+$, formed from excitations of the $[\nu p\otimes\pi h]_{1^+}$ type, has $T=T_0+1$ and $T_z=T_0+1$ ($\tau=1$, $\mu_\tau=1$) and is also referred to as a Gamow–Teller resonance with $\mu_\tau=+1$. Its energy can vary strongly from nucleus to nucleus.

From the viewpoint of the phenomenological approach, the Gamow–Teller ($\tau=1$, $\mu_\tau=-1$) resonance, the $M1$ ($\tau=1$, $\mu_\tau=0$) giant resonance, and the Gamow–Teller ($\tau=1$, $\mu_\tau=+1$) resonance form an isobaric triplet of 1^+ states. However, from the microscopic point of view these states cannot be regarded as an isobaric triplet, because, owing to the Pauli principle, the configurations forming these states do not always undergo transitions into each other when acted on by the operators T_+ and T_- (Refs. 5, 24, and 25).

Ideas about the nonstatistical structure of the strength functions $S_\beta(E)$ have turned out to be important for widely differing areas of nuclear physics.[5]

1.3. Calculation of the strength functions of beta transitions

The microscopic description of the β-transition strength functions is closely related to the analysis of astrophysical and thermonuclear processes, analysis of the values of $\log ft$ for β transitions between low-lying states, the description of delayed processes, analysis of the $M1\gamma$ decay of analog resonances, and study of the properties of the Gamow–Teller resonance.

The suppression of $0^+\Rightarrow 0^+$ Fermi β transitions is associated with the existence of a collective state—the isotopic analog of the ground state of the parent nucleus, carrying the principal strength of Fermi β transitions and located above the ground state of the parent nucleus[30] (Fig. 1). From the microscopic point of view, the collectivization of the analog is associated with the existence of the residual interaction

$$V_{\tau\tau}=\tfrac{1}{2}G_\tau(\tau_1\tau_2). \tag{8}$$

Just as the suppression of Fermi β transitions [the operator $\beta_F^\pm=\Sigma_k\tau_\pm(k)$] can be explained by taking into account the residual interaction $V_{\tau\tau}$, to explain the suppression of Gamow–Teller transitions [the operator $\beta_{GT}^\pm=\Sigma_k\tau_\pm(k)\sigma(k)$] the authors of Refs. 14, 31, and 32 introduced the residual interaction

$$V_{\tau\tau\sigma\sigma}=\tfrac{1}{2}G_{\tau\sigma}(\tau_1\tau_2)(\sigma_1\sigma_2). \tag{9}$$

The models used at present to calculate $S_\beta(E)$ can be divided into two classes.[33,34] The first contains models in which the specific shell structure of the nucleus is ignored, but the damping of giant resonances associated with $[\pi p$

$\otimes \nu h]_{1^+}$ and $[\nu p \otimes \pi h]_{1^+}$ configurations is approximately taken into account. The most frequently used such models are:

1. The gross theory,[35,36] in which all the particle–hole configurations forming $S_\beta(E)$ are assumed to be degenerate in energy.

2. The schematic model,[37,38] in which all the particle–hole transitions are divided into energy groups depending on the spin flip, and the basic relations are obtained by semiclassical summation in the theory of finite Fermi systems.

These models possess an important advantage: they allow a parameter-dependent analytic description of the resonance characteristics. However, they cannot describe phenomena in detail.

The second group includes models using a realistic basis of shell configurations and an effective quasiparticle interaction parametrized in some given form. The most commonly used such models are:

1. Models[5,14,39,40] in which the Tamm–Dancoff approximation or the random-phase approximation is used to diagonalize the shell-model Hamiltonian on the particle–hole basis, neglecting the single-particle continuum and the coupling of simple configurations to complex ones, which leads to the appearance of δ peaks in $S_\beta(E)$. Models of this type have been used successfully to calculate $S_\beta(E)$ for intermediate and heavy nuclei.[14,31] The residual spin–isospin interaction leads to the appearance of a state in whose wave function the basis particle–hole configurations enter coherently (i.e., with the same sign). This state is identified as the Gamow–Teller resonance. Resonance relaxation is included by broadening the δ peaks, using Gaussian or Breit–Wigner distributions.[5,41,42]

2. Models[43,44] in which $S_\beta(E)$ is described by the shell model taking into account the particle–hole continuum and effective nucleon–nucleon interactions in the particle–particle and particle–hole channels. The widths of the maxima, due only to the nonzero probability for nucleon emission into the continuum ($\Gamma \approx 100$ keV; Refs. 34 and 45), turn out to be much smaller than the observed ones (1 MeV; Refs. 5 and 28), which makes it necessary to add a complex term to the energy in the particle–hole propagator. Then the energy widths of the peaks in charge-exchange processes are described satisfactorily.

3. The quasiparticle–phonon model,[28,46] based on diagonalizing the Hamiltonian on a basis including both particle–hole $(1p,1h)$ and $(2p,2h)$ configurations, which allows the effective inclusion of the peak relaxation in $S_\beta(E)$, i.e., estimation of the peak width.[47] The neglect of the single-particle continuum in this model somewhat limits its range of applicability and makes it difficult to study a number of nuclear reactions.

4. The optical-shell model,[34,48] which includes the nuclear shell structure, the effects of the single-particle continuum, and the coupling of particle–hole configurations forming resonances in $S_\beta(E)$ to multiparticle configurations. The coupling of particle–hole and multiparticle configurations is described within a particular parametrization of the optical model. The quasiparticle damping is analyzed in terms of the imaginary part of the optical potential.

It should be noted that the existing models for calculating $S_\beta(E)$ are not capable of completely describing β decay. However, they can be used to obtain a fairly good description of the locations and relative intensities of the peaks in $S_\beta(E)$, which is completely sufficient for, for example, describing delayed processes. New experimental data on $S_\beta(E)$ will undoubtedly stimulate the further development of microscopic approaches to calculating the strength functions. The calculations can be improved by using different variants of the $(1p,1h)$ basis and systematically including the coupling of these configurations to multiparticle ones, and also using different variants of the effective interaction.

Some of the first microscopic calculations of $S_\beta(E)$ for Gamow–Teller β transitions in several nuclei taking into account shell effects were performed by the Tamm–Dancoff method (the TDA model).[5,14] We shall discuss this model in more detail, since both the model itself and the fundamental principles on which it is based are used in many current studies.[49,50] The Hamiltonian of the system is written as the sum of the single-particle part (H_{sp}) of the shell model and charge-exchange residual interactions:

$$H = H_{sp} + V, \tag{10}$$

where the residual interactions have the form [see (8) and (9)]

$$V = V_{\tau\tau} + V_{\tau\tau\sigma\sigma},$$

$$G_{\tau\tau} = (1.0\text{–}1.5) G_{\tau\sigma}. \tag{11}$$

The states obtained from the parent state $|\Psi_0\rangle$ by acting on it with the β-decay operator are used as the basis functions. Then the matrix elements of the interaction V are represented in factorized form:

$$\langle f|V|f'\rangle = \frac{G}{2} V_f V_f, \tag{12}$$

where the V_f turn out to be proportional[5] to the amplitudes for β transitions to basis states $|f\rangle$ having excitation energy E_f.

For example, for the Gamow–Teller β decay of an N-odd nucleus, the basis states include single-particle proton states $|j_{p1}\rangle$ and three-quasiparticle states $|[j_{n1} \otimes (j_p \otimes j_{n^-})_{1^+}]_J\rangle$ with spin $J = j_{n1}, j_{n1} \pm 1$.

For the β decay of a Z-odd nucleus with the odd proton in the state $|j_{p1}\rangle$, the basis states include single-particle neutron states $|j_{n1}\rangle$ and three-quasiparticle states $[j_{p1} \otimes (j_n \otimes j_{p^-})_{1^+}]_J$, $J = j_{p1}, j_{p1} \pm 1$.

Diagonalization of the matrix

$$H_{ff'} = E_f \delta_{ff'} + G_{\tau\sigma} V_f V_{f'} \tag{13}$$

gives the energies and wave functions of the states of the daughter nucleus populated in Gamow–Teller β transitions and allows $S_\beta(E)$ and $T_{1/2}$ to be determined.[5,14]

The strength functions of β^+ and β^- decays differ fundamentally. In those of β^- decay the principal maximum is located near the analog. In those of β^+ decay the location of the maximum cannot be associated with the analog location, because in nuclei with $T_z > 0$ $(N > Z)$ there is no analog state relative to β^+ decay. The main difference is that the excita-

tion energies of the basis states are measured from the ground state of the daughter nucleus, and the results of the calculations for β^+ decay are more sensitive to the choice of the average field and the inclusion of various correlations.[5]

Models using the QRPA[51,52] have been widely used in recent years to calculate $S_\beta(E)$. In the approaches based on the QRPA, the wave functions are constructed on the basis of a given single-particle model with pairing and residual interaction of the charge-exchange type, which is treated in the random-phase approximation.[39,40,51]

The typical value of the Gamow–Teller residual interaction constant is (Refs. 5, 14, 39, and 51) $G_{\tau\sigma}=(40-50)/A$ MeV.

The location of the Gamow–Teller resonance for nuclei near ^{208}Pb in the QRPA model corresponds to residual interaction constant[5] $G_{\tau\sigma}=46/A$ MeV. The calculated location of the Gamow–Teller resonance varies by 12% as $G_{\tau\sigma}$ varies by 40% (Ref. 52). The location of the other resonances in $S_\beta(E)$ is less sensitive to the choice of the constant $G_{\tau\sigma}$.

Let us make a few comments about the strength functions of β^- and β^+ transitions. The strength functions S_β of these transitions differ qualitatively, as is clearly seen in the full sum of β^+ and β^- transitions. For Gamow–Teller β^- transitions we have the sum rule[18,29]

$$S_- - S_+ = 3(N-Z), \tag{14}$$

where

$$S_\pm = \sum_i B_\pm(\mathrm{GT},E_i), \tag{15}$$

and the $B_\pm$ are related to S_β by Eqs. (4)–(6).

The quantities $S_\pm$ are called the integrated strengths of Gamow–Teller excitations in the β^- or β^+ decay channels. The sum rule (14) is model-independent in the space of the nucleon degrees of freedom, i.e., it must hold when various nucleon correlations are present, but may be modified when non-nucleon degrees of freedom are included (quarks, baryon resonances, and so on). It follows from (14) that in nuclei with $N>Z$, the full sum of β^- transitions is considerably larger than that of β^+ transitions. However, this does not imply that $\log ft$ must strongly differ for β^- and β^+ transitions, since by no means do all the states contributing to $S_\pm$ lie in the energetically allowed window ($E<Q_\beta$) (Fig. 1). For example, more than 90% of the full strength of Gamow–Teller β^- transitions is concentrated in the Gamow–Teller resonance, whose excitation energy is higher than Q_β, so that the strengths S_+ and S_- at low excitation energies can be comparable.[5]

In $S_\beta(E)$ for β^- transitions, the principal maximum is located near the analog state (Fig. 1). The location of the principal maximum in $S_\beta(E)$ for β^+ (EC) decay can vary greatly in going from one nucleus to another. However, whereas the principal maximum in S_{β^-} ($\mu_\tau=-1$) is in principle unattainable in the β^- decay of nuclei with $N>Z$, the Gamow–Teller resonance with $\mu_\tau=+1$ can fall below Q_β for some nuclei[50] and be manifested in β^+ (EC) decays. In nuclei with $Z>N$ the situation regarding β^+ and β^- decays is reversed.

The differences between S_{β^+} and S_{β^-} have little effect on the probabilities of β^+ and β^- transitions in nuclei near the stability band. These differences are manifested more strongly in going away from the β-stability band and with increasing total β-decay energy Q_β.

1.4. The Fermi function

Let us briefly discuss the calculations of the Fermi functions, which are needed for analyzing the experimental data and for comparing theory and experiment (3).

The β-decay probability per unit time is written as[16]

$$W_{fi}=\frac{2\pi}{\hbar}|H_{fi}|^2\frac{dk_e dk_\nu}{(2\pi)^6}\delta(E_0-\varepsilon_e-E_\nu), \tag{16}$$

where E_0 is the total β-decay energy, H_{fi} is the matrix element of the β transition from the initial state (i) to the final state (f), k_e and E_e are the electron wave vector and energy, and k_ν and E_ν are the antineutrino wave vector and energy. The matrix element $|H_{fi}|$ contains the product of the nuclear matrix element $|M_{fi}|$ and the density of states for the electron and antineutrino. As a result, for the electron energy distribution we can write[16,53]

$$\frac{dW_{fi}}{d\varepsilon}=\frac{m_e c^2}{\hbar}\frac{\Gamma^2}{\pi^3}\rho(\varepsilon,Z,R)|M_{fi}|^2(\varepsilon_0-\varepsilon)^2\varepsilon(\varepsilon^2-1)^{1/2}, \tag{17}$$

where $\varepsilon=E_e/m_e c^2$, $\varepsilon_0=E_0/m_e c^2$, $B\equiv(\hbar/m_e c^2)\times(2\pi^3\ln 2/\Gamma^2)=4131$ sec, and the function $\rho(Z,R,\varepsilon)$ describes the effect of the atomic electric field on the energy distribution of the β particles. For allowed β transitions the effect of the atomic field on the energy distribution of the β particles is described by the Fermi function, which must be multiplied by the β spectrum calculated at $Z=0$. The total β-decay probability is[5,52]

$$W_{fi}=\frac{m_e c^2}{\hbar}\frac{\Gamma^2}{2\pi^3}|M_{fi}|^2 f(Z,R,\varepsilon_0), \tag{18}$$

where

$$f(Z,R,\varepsilon_0)=\int_1^{\varepsilon_0}\rho(Z,\varepsilon,R)(\varepsilon_0-\varepsilon)^2\varepsilon(\varepsilon^2-1)^{1/2}d\varepsilon \tag{19}$$

is the integrated Fermi function. Tables of Fermi functions have been compiled.[16,54]

The half-life is

$$T_{1/2}=\frac{\ln 2}{\Sigma W_{fi}}=\frac{\hbar}{m_0 c^2}\frac{2\pi^3\ln 2}{\Gamma^2}\left\{\sum|M_{fi}|^2 f(Z,R,\varepsilon_0)\right\}^{-1}$$
$$=\left\{\sum S_\beta(E_f)f(Z,R,\varepsilon_0)\right\}^{-1}, \tag{20}$$

where

$$S_\beta(E)=\frac{|M_{fi}|^2}{B},\quad B\equiv 4231\ \mathrm{sec}\equiv D\frac{g_v^2}{g_a^2}\equiv\frac{\hbar 2\pi^3\ln 2}{m_0 c^2\Gamma^2},$$

$$D\equiv\frac{2\pi^3\hbar^7\ln 2}{g_v^2 m_0^2 c^4}$$

[Refs. 5 and 52; see also (4)].

These expressions are valid for both β^- and β^+ decays. For electron capture, the expressions are slightly modified:[16,53]

$$E_0^{EC}=E_0^{\beta^+}+2m_0C^2-B_e, \tag{21}$$

where E_0^{EC} is the total energy of electron capture and B_e is the electron binding energy, i.e., electron capture can occur when β^+ decay is energetically forbidden. The relation between β^+ decay and electron capture depends on the transition energy.

The probability for electron capture from the K shell is

$$dW_{fi}^{(K)}=\frac{2\pi}{\hbar}|H_{fi}^{(K)}|^2\frac{dk_\nu}{(2\pi)^3}\delta(E_0-E_\nu), \tag{22}$$

$$W_{fi}^{(K)}=\frac{m_eC^2}{\hbar}\frac{\Gamma^2}{\pi}\left(\frac{\hbar}{m_eC}\right)^2\rho_k(Z,\varepsilon,R)|M_{fi}|^2\varepsilon_\nu^2, \tag{23}$$

$$T_{1/2}=\frac{\ln 2}{\Sigma(W_{fi}^{\beta}+W_{fi}^{(K)})}. \tag{24}$$

For a more accurate description of some processes (such as delayed fission), it is often important to include electron capture from the L shell:

$$W_{fi}^{k+L\,I}=\frac{m_eC^2\Gamma^2}{\hbar\pi}|M_{fi}|^2\frac{1}{4\pi}(g_{-1,k}^2q_k^2-g_{-1,L\,I}^2q_{L\,I}^2), \tag{25}$$

$$W_f^{k+L_I}=\frac{m_eC^2\Gamma^2}{\hbar 2\pi^3}|M_{fi}|^2f_{fi}^{k+L\,I}(Z,R,\varepsilon), \tag{26}$$

$$f_{fi}^{k+I}(Z,R,\varepsilon)=\frac{\pi}{2}(g_{-1,k}^2q_k^2-g_{-1,L\,I}^2q_{L\,I}^2), \tag{27}$$

where q_x is the energy carried off by the neutrino. Various tables[16,54] have been compiled for the functions f and g.

The functions g and f are calculated using the self-consistent Hartree–Fock–Slater potential for the field produced by the atomic electrons, and the effects of screening and the finite size of the nucleus are included. As a rule, the integrated Fermi functions $f(\varepsilon,Z,R)$ calculated in different ways differ by several percent, and only in exotic cases (large $Q_\beta>10$ MeV and large $Z>80$) can the differences reach 20%.

For allowed transitions it is convenient to split the integrated Fermi function for β^- and β^+ transitions into two factors:

$$f(E,Z,R)=\Phi(E)F_0(E,Z,R), \tag{28}$$

where

$$\Phi(E)=(E^2-1)^{1/2}(2E^4+9E^2-8)/60+E\ln[E+(E^2-1)^{1/2}], \tag{29}$$

and E is the total energy of the β particle, including the rest mass in units of m_ec^2. The function $\Phi(E)$ depends rather strongly on energy and is calculated analytically, while the function $F_0(E,Z,R)$ is calculated numerically; it is weakly energy-dependent and convenient for interpolation. It is the function $F_0(E,Z,R)$ which is often given in tables.

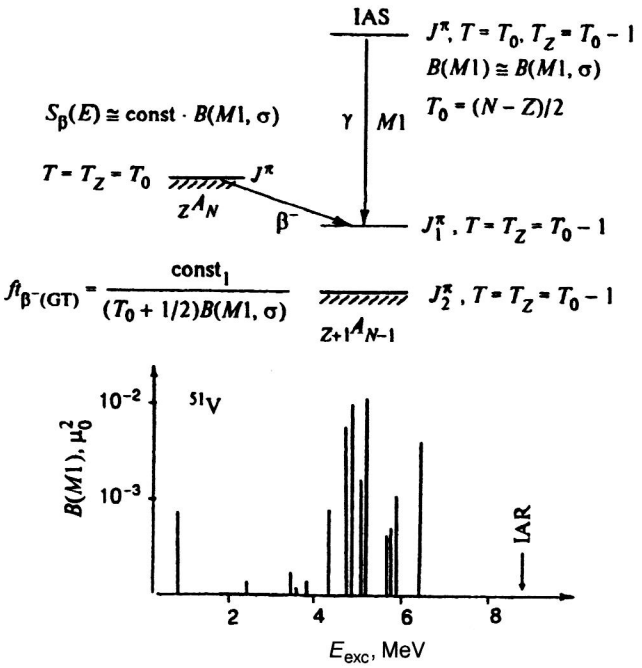

FIG. 2. Relations between the reduced probabilities $B(M1)$ for $M1\,\gamma$ transitions from the analog state and the values of ft and $S_\beta(E)$ for Gamow–Teller β^- decay. $B(M1,\sigma)$ denotes the reduced probability of the $M1\,\gamma$ transition when the l part of the $M1\,\gamma$-transition operator can be neglected. A typical experimental distribution of $B(M1)$ for the $M1\,\gamma$ decay of analogs near $A=51$ is shown.

1.5. Experimental studies of the structure of the beta strength functions and comparison with the theoretical calculations

Information about the structure of the β-transition strength functions can be obtained from the total-absorption spectra of the γ rays accompanying β decay,[5,55] from studies of the emission of delayed neutrons, protons, and α particles,[5,56–59] and by studying the $M1\,\gamma$ decay of analog resonances.[21]

The first experimental manifestations of the resonance structure of $S_\beta(E)$ were found in studying the $M1\,\gamma$ decay of analog resonances.[21] The relation between $B(M1,\sigma)$ for γ transitions from the analog state and the value of ft of the corresponding β transition (Fig. 2) is used. The isovector part of the $M1\,\gamma$ transition operator is

$$\mathfrak{M}(M1)=(3/4\pi)^{1/2}\frac{e\hbar}{2MC}(-4.7\sigma_\mu+l_\mu)t_z. \tag{30}$$

When the contribution of the orbital part (l_μ) to the $M1\,\gamma$ transition is small and can be neglected, the reduced probability of the $M1\,\gamma$ transition is denoted as $B(M1,\sigma)$. The analog state does not contain significant admixtures of states with other values of the isospin and the γ transition is purely isovector, and so we can write[6]

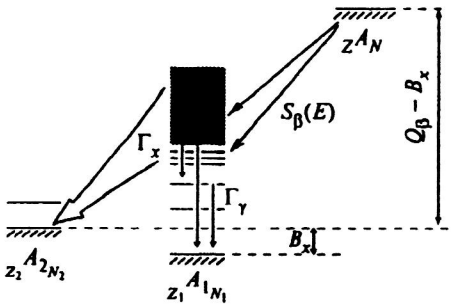

FIG. 3. Energy relations for delayed-particle emission.

$$ft=\frac{11000}{(T_0+1/2)B(M1,\sigma)},$$

$$B(M1,\sigma)\approx B(M1). \tag{31}$$

A typical distribution of $B(M1)$ for the $M1\,\gamma$ decay of analogs near $A\cong 50$ is given in Fig. 2 (Refs. 6 and 60). The $B(M1)$ distributions have a purely nonstatistical (resonance) behavior, which, according to (3) and (31), indicates that $S_\beta(E)$ is nonstatistical in nature. The model calculations of the $M1\,\gamma$ decay of analog resonances correctly describe the main qualitative characteristics of γ decay and the locations of the maxima in $S_\beta(E)$. However, the experimental and theoretical absolute values of the transition intensities are observed to differ by several times.[60]

If the energy of level i populated by the β transition exceeds the proton or α-particle separation energy, delayed protons or α particles can be emitted in the decay of that level.[58] The energy of the delayed particles is given by (Fig. 3)

$$E_i=B_x+E_f+\frac{A}{A-M_x}E_x;\quad x\equiv\begin{Bmatrix}p\\ \alpha\end{Bmatrix},$$

$$M_p=1,\quad M_\alpha=4, \tag{32}$$

where B_x is the binding energy of particle x in the daughter nucleus, E_x is the particle energy, and E_i and E_f are the energies of the initial and final states after particle emission. Several hundred emitters of delayed protons and α particles have now been discovered.[61,62] Delayed protons can be emitted after the β^+ (EC) decay of neutron-deficient nuclei. The emission of α particles is possible[62] both after the β^+ (EC) decay of neutron-deficient nuclei (^{114}Cs–^{120}Cs) and after the β^- decay of neutron-rich nuclei (^{212}Bi, ^{214}Bi, ^{16}N). Let us consider the relation between the shape of the delayed-proton spectrum and S_β (Ref. 58):

$$I_p(E_p)=\sum I_\beta(E_i)\Gamma_p^{if}/\Gamma^i, \tag{33}$$

where I_x is the emission intensity of the corresponding particle, Γ_p is the proton width, Γ is the total width, and

$$I_\beta=\text{const}\ \ S_\beta(E_i)f(Q_\beta-E_i). \tag{34}$$

If we assume that the widths Γ_p/Γ^i are uncorrelated with the β-transition probabilities and that the widths Γ_p and Γ^i can be calculated using the statistical model,[63] then

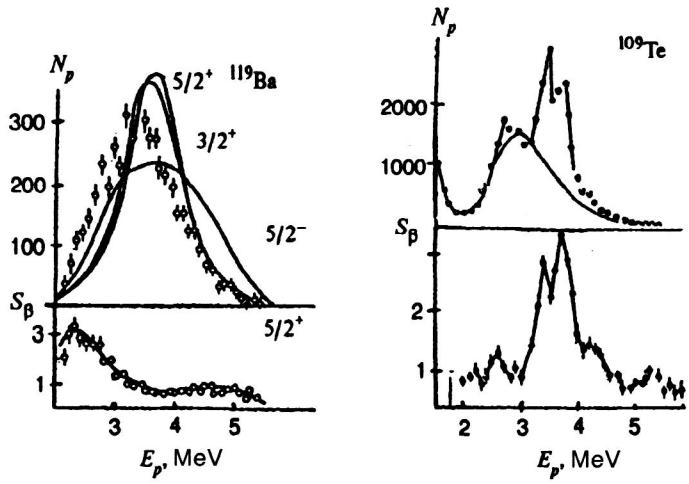

FIG. 4. Delayed-proton spectra of ^{119}Ba and ^{109}Te. The solid line is the spectrum calculated in the statistical model for various quantum numbers of the ^{119}Ba ground state. The strength functions of β^- transitions corresponding to the delayed-proton spectra are given in the lower figures.

$$I_p(E_p)=\text{const}\ \ S_\beta(E_i)f(Q_\beta-E_i)G(E_p), \tag{35}$$

where $G(E_i)=\langle\Gamma_p(E_p)/\Gamma(E_i)\rangle$ is the statistical average of the ratio $\Gamma_p(E_p)/\Gamma(E_i)$. The function f in (31) falls off according to a power law for $E_p\to Q_\beta$, while the function $G(E_p)$ falls off exponentially for $E_i\to B_p$, and the delayed-proton spectrum has the characteristic bell shape with width 2–3 MeV (Ref. 58). Therefore, a fairly narrow range of $S_\beta(E)$ can be judged from the delayed-proton spectra. The spectrum of delayed α particles has a similar shape, but its maximum is shifted to lower energies, owing to differences in the separation energies and the Coulomb barriers.

Therefore,

$$S_\beta(E_i)=\text{const}\ \ I_x(E_i)/R(E_i). \tag{36}$$

The function $R(E)$ depends strongly on the parameters of the model used to calculate $\langle\Gamma_x(E)/\Gamma(E)\rangle$, but this expression can be used as a qualitative estimate of $S_\beta(E)$. If the resonance in $S_\beta(E)$ lies in the range from B_x up to Q_β, this must essentially be reflected in the shape of the delayed-particle spectrum. The first manifestations of the resonance structure of $S_\beta(E)$ in the delayed-proton spectra were discovered in Refs. 58 and 64. As a rule, the spectra of delayed protons or α particles are not very sensitive to the choice of $S_\beta(E)$, and good agreement with experiment can be obtained by an appropriate choice[58] of the model parameters in calculating $\langle\Gamma_x/\Gamma\rangle$. That is, experiment is about equally sensitive to the shape of $S_\beta(E)$ and to the model for calculating $\langle\Gamma_x/\Gamma\rangle$. However, for some nuclei it is impossible to describe the experimental data without the resonance structure of $S_\beta(E)$, no matter how the parameters of the model for calculating Γ_x and Γ are varied.[5,58] In Fig. 4 we give the spectrum of delayed protons for ^{109}Te and the spectra calculated by using various shapes of $S_\beta(E)$. It follows from this figure that the delayed-proton spectrum of ^{109}Te can be described only by including the resonance structure of $S_\beta(E)$. We encounter the same situation for ^{121}Ba and ^{114}Cs (Refs. 5 and 58).

By studying the delayed-neutron spectra it is possible to obtain more detailed information about the structure of $S_\beta(E)$ than by studying delayed protons or α particles, owing to the absence of the Coulomb barrier. The probabilities for emitting delayed neutrons in the β^- decay of neutron-deficient nuclei turn out to be significantly higher than those for emitting protons or α particles after the β^+ (EC) decay of neutron-deficient nuclei at the same values of $(E_i - B_x)$ (Fig. 3). The absence of the Coulomb barrier makes it possible to obtain information about $S_\beta(E)$ in a wider energy range, namely, practically from the neutron binding energy in the daughter nucleus B_n up to Q_β.

Manifestations of the resonance structure of the strength functions $S_\beta(E)$ in the delayed-neutron spectra have been observed for many nuclei.[26,65]

For nuclei with a rather large neutron excess, states of the backward spin-flip and core-polarization type are populated in β^- decay. As noted in Ref. 5, these states can also appear in delayed-neutron spectra. By now, several hundred emitters of delayed neutrons have been identified.[99] The probabilities for populating level i in β^- decay I^i_β and emitting a delayed neutron $I_n(E)$ of energy $E = E_i - B_n - E_f$ are related as[5,58]

$$I^i_\beta = \sum \frac{\Gamma^i}{\Gamma^i_n} I_n(E_i - B_n - E_f), \tag{37}$$

where Γ^i is the total width of the level, $\Gamma^i \approx \Gamma^i_\gamma + \Gamma^i_n$, and Γ^i_n is the neutron width of the level. Equation (37) can be inverted:

$$I^f_n(E) = \sum I^i_\beta(E_i) \frac{\Gamma^i_n}{\Gamma^i}. \tag{38}$$

The widths Γ^i and Γ^i_n are calculated using the statistical model,[58,66] and the intensity $I^i_\beta(E_i)$ is related to the β-decay strength function by (3).

An example[67,68] of the strength function for the β^- decay of ^{95}Rb, obtained by analyzing the delayed-neutron spectrum, is given in Fig. 5, where we also give the results of calculating $S_\beta(E)$ using various models. Comparing the experimental[67] and theoretical[5,68] data, we see that the delayed-neutron spectrum can be correctly described only by taking into account nonstatistical effects in $S_\beta(E)$. A similar situation occurs for many other emitters of delayed neutrons.[26,65,69]

A characteristic feature of the strength functions of the β^- decays of many nuclei obtained by analyzing the delayed-neutron spectra is their resonance behavior. The nature of these resonances is explained in Refs. 5 and 65. The maxima near Q_β are associated with transitions to states of the core-polarization type, while the lower-lying peaks are associated with transitions of the backward spin-flip type, introduced into the TDA calculations in Refs. 5 and 14.

We note that in purely statistical calculations with modeling of different types of fluctuations, it is possible in principle to obtain "peaks" in the delayed-neutron spectra,[70] but impossible to describe the regularities in the intensities and locations of the peaks when studying various nuclei.[5] The regularities in the resonance structure of $S_\beta(E)$ can be explained only by using the nonstatistical properties of $S_\beta(E)$.

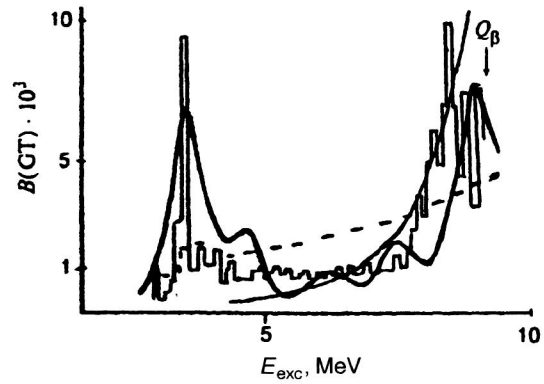

FIG. 5. Strength function for the β^- decay $^{95}\text{Rb} \xrightarrow{\beta^-} {}^{95}\text{Sr}$: theoretical calculations using various models and experimental data from analysis of the delayed-neutron spectra. The histogram is from experiment, the thin solid line is the calculation using the statistical model [$S_\beta(E) \simeq \rho(E)$], the dashed line is the calculation using the gross theory, and the heavy solid line is for $S_\beta(E)$ calculated using the microscopic model including the Gamow–Teller residual interaction.

Some studies quote data only on the delayed-neutron emission probability, i.e., the probability for emitting a delayed neutron per β^--decay event:

$$P_n = \frac{\int_{B_n}^{Q_\beta} S_\beta(E) f(Q_\beta - E) \frac{\Gamma_n}{\Gamma_{\text{tot}}} dE}{\int_{B_n}^{Q_\beta} S_\beta(E) f(Q_\beta - E) dE}. \tag{39}$$

The value of P_n varies from a fraction of a percent to tens of percent[65] and is sensitive to the shape of the β-decay strength function.[15,65]

Before comparing the experimental and theoretical values of P_n, let us make one remark regarding the calculation of probabilities for delayed processes. The calculated probabilities for delayed processes are rather unreliable when the parameters determining the energetics of the process (B_x, Q_β, and so on) are poorly known. This has an especially strong effect on calculations of P_n when there are peaks in $S_\beta(E)$ near Q_β or B_n. For example, in calculating P_n for ^{31}Na (Ref. 52), reasonable variations of the mean-field parameters cause the location of the peak in $S_\beta(E)$ to vary from 1.94 MeV to 2.06 MeV, i.e., they raise it just above B_n ($B_n \simeq 2$ MeV). This causes P_n to increase by 75%, while the half-life changes by only 2% altogether. A similar situation occurs for all delayed processes, in particular, for the delayed fission of nuclei far from the stability band. Therefore, theoretical calculations of the probabilities for delayed processes must be treated with care for nuclei far from the β-stability band.[71]

It can thus be stated that the probability for delayed-neutron emission can be described only when the structure in $S_\beta(E)$ is taken into account. However, it is not always possible[5,52] to obtain detailed agreement between the theoretical and experimental values of P_n. In the opinion of the authors of Ref. 5, there are two reasons for this. The first is that it is necessary to use $S_\beta(E)$ with the real widths of the

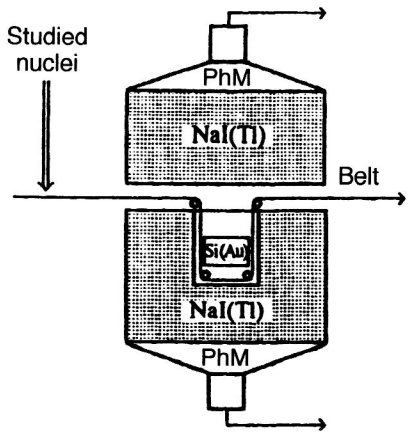

FIG. 6. Experimental setup for measuring the γ-ray total-absorption spectra. After mass separation, the studied nuclei are transported to a well in the NaI(Tl) crystal, where the β detector is located. The total-absorption spectra are measured in 4π geometry, both with and without coincidence with β particles.

peaks, and reliable calculation of the latter is quite problematical. The second, perhaps more important, reason is that the widths Γ_n and Γ_{tot} are calculated using the statistical model, which, in general, can only be an approximation. Therefore, the data on $S_\beta(E)$ obtained from the delayed-particle spectra and the delayed-particle emission probabilities can be viewed as estimates. More rigorous and detailed conclusions can be drawn by studying β decay or nuclear reactions directly.

A conclusion about the nonstatistical nature of $S_\beta(E)$ can be drawn on the basis of measuring $S_\beta(E)$ by the γ-ray total-absorption method (Refs. 5, 27, 28, and 72). This method is attractive because it allows information to be obtained about the structure of $S_\beta(E)$ in direct experiments. The operating principle of a total-absorption spectrometer is based on summation of the energies of the cascade γ rays produced after β decay to excited levels of the daughter nucleus in 4π geometry. The first successful experiments[5,27,55] performed using a total-absorption spectrometer showed that resonance structure of $S_\beta(E)$ is a typical feature of nuclear β decay. At present, γ-ray total-absorption spectrometers are being used in many experiments to study the characteristics of $S_\beta(E)$ (Refs. 28, and 72–74).

Let us discuss the analysis of the γ-ray total-absorption spectra for the example[28] of the β^+ (EC) decay of ^{147g}Tb ($T_{1/2}=1.6$ h). The ^{147g}Tb sources were obtained by bombarding a tantalum target by a 660-MeV proton beam. Thirty minutes after the bombardment the target was dissolved and the Tb fraction was extracted by the chromatography method. The ^{147}Tb nuclei were isolated from the Tb fraction by mass separation at the YaSNAPP-2 complex,[75] implanted on Al foil, and studied using a γ-ray total-absorption spectrometer (Fig. 6). The efficiency ε_{tot} of recording γ rays in the energy range 0.6–4.2 MeV by using the total-absorption peak depends exponentially on the summed energy of the γ transitions, E_γ (Ref. 28):

$$\varepsilon_{\text{tot}}=\exp(-0.78E_\gamma), \tag{40}$$

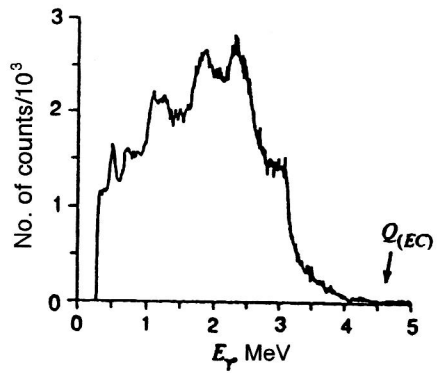

FIG. 7. γ-ray spectrum from ^{147g}Tb decay measured with a total-absorption spectrometer in coincidence with β^+ particles. The arrow indicates the total energy of electron capture for ^{147g}Tb.

where E_γ is expressed in MeV. It is well known[5] that in this case the intensity of the γ-ray total-absorption peak is proportional to the level-population probability in β decay and independent of the decay scheme. The spectral analysis reduces to isolating the total-absorption peaks and determining their intensities. The β strength function is constructed by using the data on these intensities by means of (3). The γ spectra measured with a total-absorption spectrometer in coincidences with β^+ particles in the β^+ (EC) decay of ^{147g}Tb and also without coincidences are shown in Figs. 7 and 8. The maximum energy of the total-absorption spectra is determined by the total energy of electron capture, Q_{EC}. The peak of energy $E_\gamma\approx 4$ MeV in Fig. 8 and the peak with $E_\gamma\approx 3$ MeV in Fig. 7 have the maximum energies and are identified as total-absorption peaks. The peak with $E'_\gamma \approx 3$ MeV in Fig. 7 corresponds to the peak with $E_\gamma=E'_\gamma - 2m_ec^2\approx 2$ MeV in Fig. 8, where $2m_ec^2$ is the energy of the two annihilation quanta. Therefore, the peak of energy $E_\gamma\approx 2$ MeV in Fig. 8 is also a total-absorption peak. It is thus possible to reliably identify two peaks at 4 and 2 MeV in the strength function of the β^+ (EC) decay of ^{147g}Tb (Fig. 9), and determinination of the intensities and energies of these two peaks in analyzing the γ total-absorption spectra does not require any information about the decay scheme. A third peak at $E\approx 1.4$ MeV is observed in $S_{\beta(\text{EC})}(E)$ for

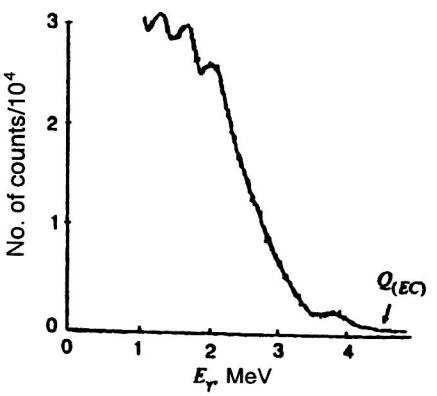

FIG. 8. γ-ray spectrum from ^{147g}Tb decay measured using a total-absorption spectrometer without coincidence with β^+ particles. The arrow indicates the total energy of electron capture for ^{147g}Tb.

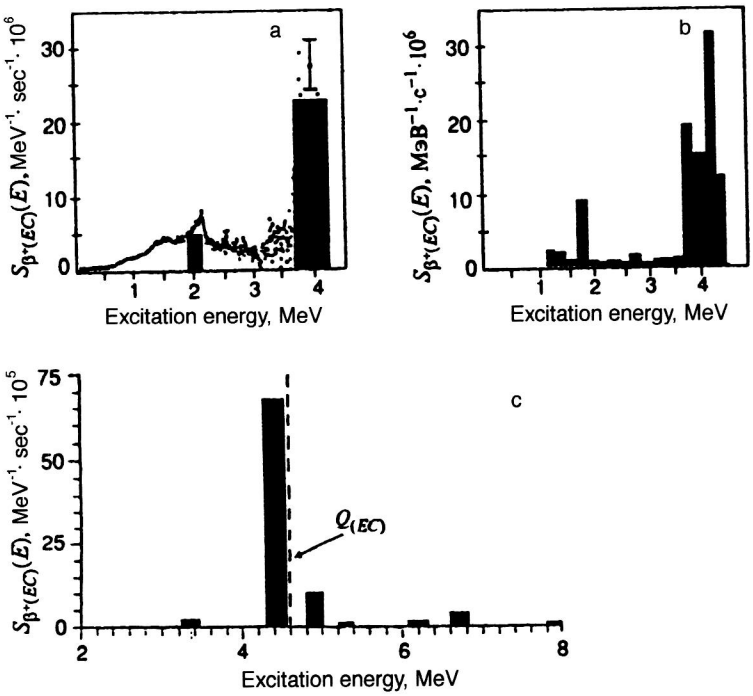

FIG. 9. Strength function of the β^+ (EC) decay of ^{147g}Tb obtained from (a) analysis of the γ-ray total-absorption spectra; (b) analysis of the ^{147g}Tb decay scheme; (c) calculation in the MQPM.

^{147g}Tb, but, owing to the difficulty of identifying the total-absorption peak in this energy range, reliable information on the intensity of this peak requires information on the ^{147}Gd decay scheme.

In Fig. 9 the intensity of the peak with $E \approx 1.4$ MeV in $S_\beta(E)$ was obtained by analyzing the γ-ray total-absorption spectra (Figs. 7 and 8), assuming level decay near excitation energy $E \approx 1.4$ MeV via two γ rays of equal energy. Therefore, in the strength function of the β^+ (EC) decay of ^{147g}Tb (Fig. 9a) it is possible to reliably determine the energies and intensities of two peaks of energy $E \approx 4$ and 2 MeV and to establish the presence of a third peak of energy $E \approx 1.4$ MeV (Ref. 28).

The ^{147g}Tb decay represents a rare case where $S_{\beta^+(EC)}$ can be constructed from the data on the decay scheme. The function $S_{\beta^+(EC)}$, obtained in Ref. 28 by analyzing the ^{147g}Tb decay scheme,[76] is shown in Fig. 9b. We see from Figs. 9a and 9b that the functions $S_{\beta^+(EC)}$ obtained by the two different methods are in good agreement with each other, indicating that $S_{\beta^+(EC)}$ is reliably determined from the total-absorption spectra in those cases where $S_{\beta^+(EC)}$ contains a small number of peaks. The calculations of Ref. 28 using the QRPA (Fig. 9c) predict the presence of the most intense peak in $S_\beta(E)$ (a Gamow–Teller resonance with $\mu_\tau = +1$) near excitation energy $E \simeq 4$ MeV, which agrees with experiment. The experimental data (Fig. 9b) reveal the fine structure of this resonance.[77]

The nature of the structure of $S_\beta(E)$ is closely related to the value of the half-life (3). Although the data on $T_{1/2}$ do not give detailed information about $S_\beta(E)$, the half-lives can be determined fairly reliably experimentally, and the theoretical values of $T_{1/2}$ depend on the model used to calculate $S_\beta(E)$ (Refs. 5 and 39).

The first qualitative explanations of the systematic retardation of Gamow–Teller β transitions were given within the gross theory,[40] where the principal strength of Gamow–Teller-type excitations is concentrated near the Gamow–Teller resonance, and the rest of $S_\beta(E)$ is approximated by a smooth function.

The first calculations of $T_{1/2}$ including the nuclear shell structure and the Gamow–Teller residual interaction were made using the TDA model.[5,78] Calculations in the Tamm–Dancoff approximation (TDA) give more accurate values of $S_\beta(E)$ and $T_{1/2}$ than those using the gross theory, and the results agree better with experiment.

In Ref. 39 the half-lives were calculated using the QRPA model for a large group of nuclei. Although for individual nuclei the calculations using the random-phase method including pairing (the QRPA model) give values of $T_{1/2}$ closer to experiment and, on the whole, give a more accurate description of the values of $T_{1/2}$ than the TDA model, the disagreement between their results and experiment can reach a factor of 10–50 (Fig. 10). Models which do not include the details of the shell structure of $S_\beta(E)$ (the gross theory) can give unpredictable discrepancies with experiment amounting to factors of tens to thousands, and in the overwhelming majority of cases the gross theory gives half-lives which are too large.

Thus, models which include the structure of the β-transition strength function can be used to estimate the half-lives for Gamow–Teller β transitions, but at present there is no agreement between theory and experiment in the details.

1.6. Nonstatistical effects in the beta decay of exotic nuclei

Particularly interesting information about nuclear properties can be obtained by studying the structure of $S_\beta(E)$ for nuclei very far from the β-stability band. The reasons for this are the following.

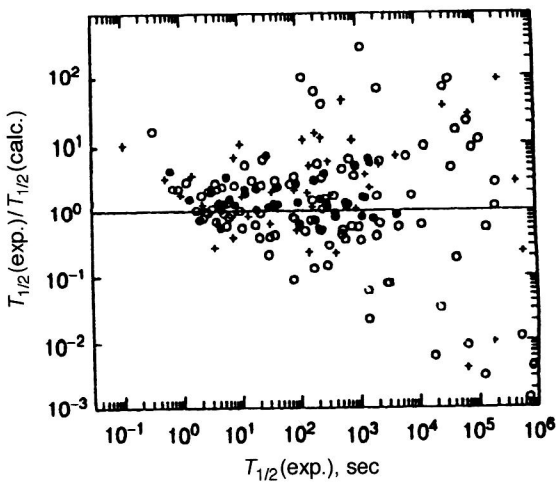

FIG. 10. Comparison of the experimental values of the half-lives of β^+ (EC) decay with the calculations including charge-exchange interactions and pairing in the QRPA: ● are even–even nuclei, ○ are odd nuclei, and + are odd–odd nuclei.

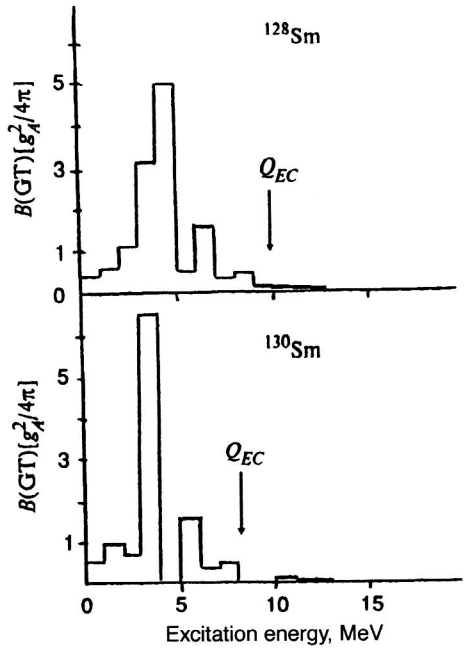

FIG. 12. Strength functions for Gamow–Teller β^+ (EC) decays of ^{128,130}Sm calculated in the TDA model.

1. Nonstatistical effects can be significantly enhanced in nuclei with a large neutron excess. This is related to the possibility of restoration of the spin–isospin $SU(4)$ symmetry with increasing $(N-Z)$ (Refs. 38 and 79) and reduction of the degree of mixing of closely spaced levels with different $SU(4)$ quantum numbers. One consequence of the spin–isospin $SU(4)$ symmetry in nuclei is equality of the energies of the isobar-analog resonance E(IAR) and the Gamow–Teller resonance E(GT). The difference of the energies of these resonances $\Delta E = E(\mathrm{GT}) - E(\mathrm{IAR})$ as a function of the neutron excess was calculated[24] and compared with experiment[23] in Ref. 5 (see Fig. 11). The line

$$E(\mathrm{GT}) - E(\mathrm{IAR}) = [-50.2(N-Z)/A + 11.0] \text{ MeV} \tag{41}$$

runs through all the calculated points. We see from Fig. 11 that the difference ΔE essentially depends on the shell structure and is described by a straight line only on the average. Obviously, on the average ΔE decreases with increasing $(N-Z)$, i.e., the spin–isospin $SU(4)$ symmetry and the related nonstatistical effects can be more clearly expressed in exotic nuclei with a large neutron excess. The restoration of $SU(4)$ symmetry will be manifested experimentally as a decrease in the widths of the distributions of the Gamow–Teller resonance and its satellites and in the details of their γ decay. In particular, by including the quantum numbers corresponding to $SU(4)$ symmetry, it may be possible to construct relations like (31) between the γ decay of the Gamow–Teller resonance and its satellites and the β decay of the neighboring nuclei, and to study manifestations of nonstatistical effects in β transitions of different degrees of forbiddenness.

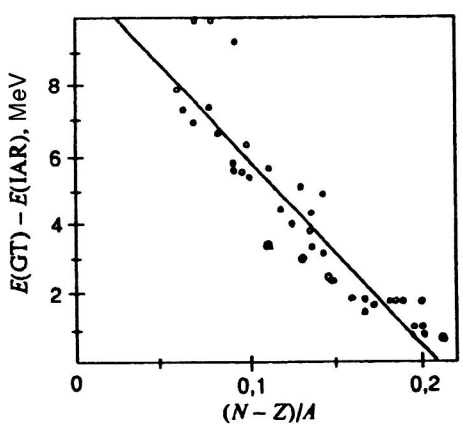

FIG. 11. Calculated location of the Gamow–Teller resonance E(GT) relative to the isobar-analog resonance E(IAR) as a function of the ratio of the difference of the numbers of neutrons and protons to the atomic number.

2. For nuclei with a large neutron deficit, it may be possible to reliably determine the total strength S_+ for β^+ (EC) decays and to analyze the sum rule (14). In fact, as the neutron deficit grows, the total energy of electron capture Q_{EC} also grows, and this in turn can cause all the peaks of the strength function $S_{\beta^+(\mathrm{EC})}(E)$ for Gamow–Teller transitions to lie in the region accessible to β^+ (EC) decay.[28,50] In Fig. 12 we give the values of $S_{\beta^+(\mathrm{EC})}(E)$ for Gamow–Teller β^+ (EC) decays of ^{128}Sm and ^{130}Sm calculated[50] using the TDA. We see from this figure that in some cases, measurement of $S_{\beta^+(\mathrm{EC})}(E)$ for nuclei with a strong neutron deficit can give information about the total strength S_+ of Gamow–Teller β^+ (EC) decays. The reliable experimental determination of S_+ and S_- is currently a problem of great interest. The reason is that the existing experimental estimates of S_+ and S_- are about 40% lower than the theoretical values (Refs. 5, 33, 34, and 50) and do not agree with the sum rule (14). However, in most cases the experimental determination of the absolute values of S_+ and S_- is not very reliable, and so we actually only have estimates of S_+ and S_- (Refs. 5 and 28).

It can therefore be expected that study of the characteristics of the beta decay of nuclei very far from the stability

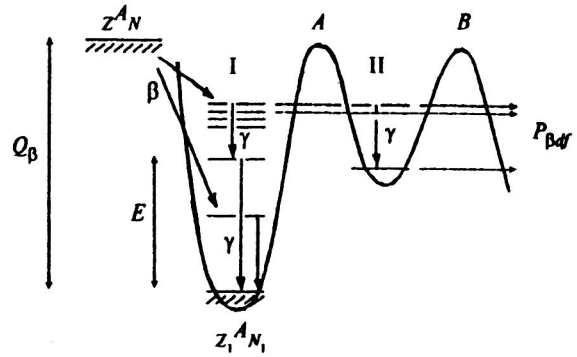

FIG. 13. Scheme of β-delayed fission (βdf). The heights of the inner (A) and outer (B) fission barriers of the daughter nucleus are indicated.

band will provide answers to a number of interesting questions about nuclear structure and properties.

The set of experimental and theoretical data discussed in this section unambiguously indicate that the strength functions of β decay must be described using the nonstatistical approach and taking into account nuclear structure. However, the theoretical models developed at present cannot give a detailed description of the experimental data on the beta decay of a wide range of nuclei. In principle, the statistical approach neglecting nuclear structure cannot adequately describe the data.

2. NONSTATISTICAL EFFECTS AND β-DELAYED NUCLEAR FISSION

2.1. β-delayed nuclear fission

The fission of nuclei from excited states populated in the β decay of the parent nucleus is called β-delayed fission.[80] This phenomenon was discovered[81,82] in the Flerov Nuclear Reactions Laboratory of the JINR in the actinide region and is now being studied for a fairly wide range of heavy nuclei.[83–91,104] By now, β-delayed fission has been discovered for many more light nuclei; in particular, Refs. 92 and 93 report the observation of β-delayed fission in the region ^{180}Tl–^{188}Bi. The study of delayed fission gives information about the nuclear fission barriers, which is important in cosmic dating and in calculating element production in astrophysical processes.

The probability of β-delayed fission $P_{\beta df}$ is determined as[14]

$$P_{\beta df}=\frac{\Sigma_i f(E_i)S_\beta(E_i)\dfrac{\Gamma_f(E_i)}{\Gamma_{tot}(E_i)}}{\Sigma_j f(E_j)S_\beta(E_j)}, \qquad (42)$$

where $f(E)S_\beta(E)$ is the probability of β decay to a level with excitation energy E, $f(E)$ is the Fermi function, $\Gamma_f(E)$ is the fission width, and $\Gamma_{tot}(E)$ is the total width. The energy relations are shown in Fig. 13. We see from (42) that to calculate the delayed-fission probability it is necessary to have information about the β strength function $S_\beta(E)$.

TABLE I. Fission-barrier parameters of ^{236}U and ^{238}U, and total β^--decay energies Q_β for ^{236}Pa and ^{238}Pa.

Daughter nucleus	E_A, MeV	E_B, MeV	E_2, MeV	$\hbar\omega_A$, MeV	$\hbar\omega_B$, MeV	Q_β, MeV
^{236}U	6.1	5.9	2.6	0.9	0.7	3.1
^{238}U	6.2	5.9	2.5	1.0	0.72	3.9

2.2. The strength functions of β^+ (EC) and β^- decays, and delayed fission of actinide nuclei

The observation of the delayed fission of ^{236}U and ^{238}U nuclei after the β^- decay of ^{236}Pa and ^{238}Pa was reported in Refs. 84–86. The parameters of the ^{236}U and ^{238}U fission barriers are well known[94] and are given in Table I. The delayed fission of ^{236}U and ^{238}U, taking into account nonstatistical effects in $S_\beta(E)$ leading to structure in the latter, was calculated in Ref. 14. The fission widths were obtained using the model of a two-hump fission barrier.[31,95] The main competing decay channel contributing to Γ_{tot} is γ emission. The γ widths were calculated following Ref. 96. The fission width was calculated as in Ref. 97.

The strength functions for the β^- decay of ^{236}Pa and ^{238}Pa are also given in Fig. 14. The function $S_\beta(E)$ for ^{236,238}Pa was calculated[14] using the shell model including the Gamow–Teller residual interaction in the Tamm–Dancoff

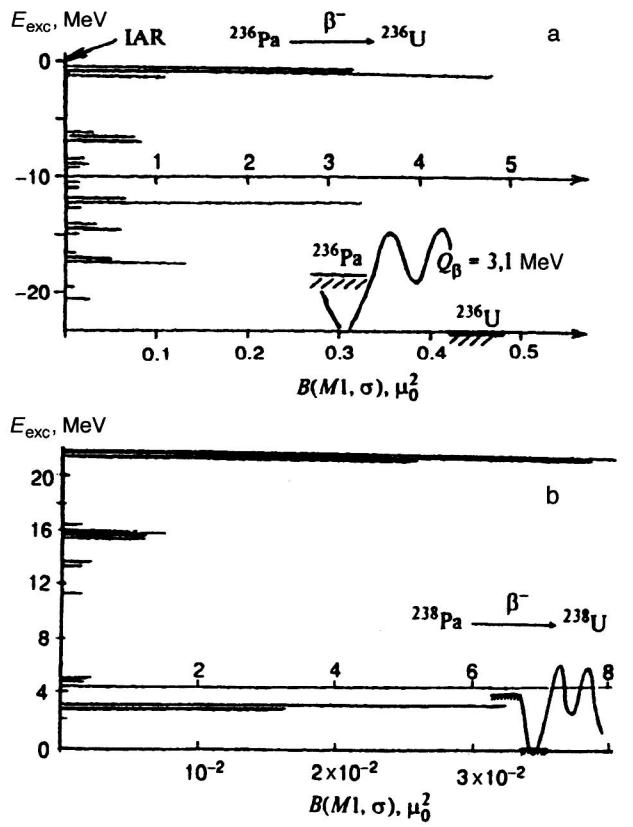

FIG. 14. Strength function $S_\beta(E)$ for β^- decay of (a) ^{236}Pa and (b) ^{238}Pa, and the ^{236,238}U fission barriers. $B(M1,\sigma)=11\,000/(T+\frac{3}{2})ft=\text{const}\cdot S_\beta(E)$, where T is the isospin of the ground state of the daughter nucleus, $B(M1,\sigma)$ is in units of μ_0^2 (μ_0 is the nuclear magneton), and ft is in seconds.

TABLE II. Delayed-fission probabilities $P_{\beta df}$ for ^{236}U and ^{238}U: experimental values and values calculated with various assumptions about the β-decay strength functions.

Nucleus	Values of $P_{\beta df}$ for various choices of S_β			
	S_β=const	$S_\beta(E)\sim\rho(E)$	TDA model	Experiment
^{236}U	$6\cdot10^{-7}$	$6\cdot10^{-4}$	10^{-12}	10^{-9}
^{238}U	$2\cdot10^{-5}$	10^{-2}	10^{-8}	10^{-8}

approximation. The principal strength of the β transitions is concentrated in the Gamow–Teller giant resonance, located near the analog state. At energies of 7–8 MeV below the analog in ^{236}U and ^{238}U there is a second maximum due to spin-flip and core-polarization transitions. At energies of about 18 MeV below the analog there is a maximum due to backward spin-flip transitions (Figs. 1 and 14)). They give the main contribution to the delayed-fission probability of ^{236}U and ^{238}U.

For ^{238}U the calculated[14] value of $P_{\beta df}$ is about 10^{-8}. For variation of the parameters determining the strength function within reasonable limits, the maximum value of $P_{\beta df}$ is about 6×10^{-8}. The experimental value of $P_{\beta df}$ for ^{238}U was also found[85] to be 10^{-8}.

For ^{236}U the calculated value[14] is $P_{\beta df}=4\times10^{-12}$. The maximum calculated value with variation of the strength-function parameters was $P_{\beta df}=5\times10^{-11}$. The experimental values of $P_{\beta df}$ were obtained in Refs. 85 and 86. According to Ref. 85, $P_{\beta df}=3\times10^{-10}-10^{-9}$. According to the data of Ref. 86, $P_{\beta df}=10^{-9}$.

In Table II we give the calculated values[14] of $P_{\beta df}$ for various assumptions about $S_\beta(E)$. Calculation of $P_{\beta df}$ using statistical models for the β-decay strength function gives values of $P_{\beta df}$ which are 2–3 orders of magnitude larger than the experimental ones in the case S_β=const, while for strength function proportional to the nuclear level density, $S_\beta\approx\rho(E)$, the values are 5–6 orders of magnitude larger for ^{236}U and ^{238}U.

Therefore, for the delayed fission of ^{236}U and ^{238}U the assumptions used in statistical models, S_β=const and $S_\beta(E)\approx\rho(E)$, give values of $P_{\beta df}$ which are significantly larger than the experimental values, while use of the non-statistical $S_\beta(E)$ reflecting nuclear structure effects leads to better agreement between the experimental and calculated values of $P_{\beta df}$ for ^{238}U. The latter calculation predicts that $P_{\beta df}$ decreases in going from ^{238}U to ^{236}U, also in agreement with the data.

The delayed fission $^{256}Es^m\xrightarrow{\beta^-}{}^{256}Fm\rightarrow\beta df$ was studied in Ref. 90. The value of the delayed-fission probability was found to be $P_{\beta df}\simeq2\times10^{-5}$, and the decay scheme of ^{256}Fm was studied. It was shown experimentally that delayed fission occurs mainly after β^- decay to the level with excitation energy $E\simeq1425$ keV, i.e., a manifestation of resonance structure in $S_\beta(E)$ in delayed fission was discovered experimentally. The calculations also predict the presence of a resonance in $S_\beta(E)$ near excitation energies $E\simeq1.5$ MeV.

A rather large fraction of delayed fission is observed[87,88] for the β^+ (EC) delayed fission of ^{232}Pu, $^{232}Am\xrightarrow{\beta^+(EC)}{}^{232}Pu\xrightarrow{\text{fission}}\beta df$: $P_{\beta df}=1.3^{+4}_{-0.8}\times10^{-2}$. The data on the delayed fission after the β^+ (EC) decay of ^{232}Am were used in Ref. 88 to find the parameters of the inner fission barrier (barrier A in Fig. 13) of ^{232}Pu. The results of Ref. 88, obtained by assuming S_β=const, give $P_{\beta df}=1.3\times10^{-2}$ for height of the inner fission barrier $E_A=5.3$ MeV, which is 1–2 MeV higher than predicted by the calculations using the Strutinsky method ($E^{th}=3.5$–4.3 MeV; Refs. 98 and 99). In Ref. 88 it was concluded on this basis that the "experimental" and theoretical values of the fission barriers for ^{232}Pu disagree with each other. However, as was shown in Refs. 5 and 32, the choice S_β=const is not justified and does not reflect the features of the β^+ (EC) decay in the particular case of the ^{232}Am nucleus.

The structure of the strength function of the β^+ (EC) decay of ^{232}Am was calculated in Ref. 32 on the basis of the idea of Gamow–Teller charge-exchange excitations. The single-particle states were calculated as in Ref. 100, and S_β was obtained in the Tamm–Dancoff approximation and is shown in Fig. 15. Nonstatistical effects leading to the presence of resonance structure in $S_\beta(E)$ significantly change the analysis of the values of $P_{\beta df}$. The value of the total energy of β^+ (EC) decay, $Q_\beta=5.2$ MeV, is marked by the arrow in Fig. 15 and was obtained by using the Garvey–Kelson mass

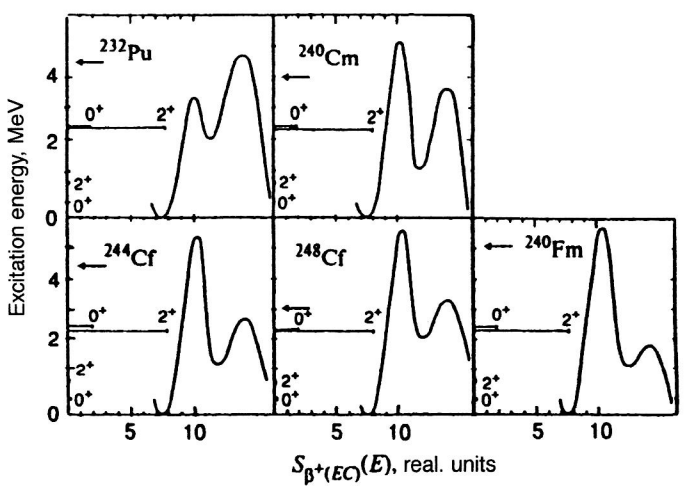

FIG. 15. Structure of the strength functions of β^+ (EC) decay of ^{240}Am, ^{240}Bk, ^{244,248}Es, and ^{248}Nd, and fission barriers of ^{232}Pu, ^{240}Cm, ^{244,248}Cf, and ^{248}Fm. The total energies of EC decay were calculated using the Garvey–Kelson mass formulas[101] and are indicated by the arrows.

TABLE III. Experimental and theoretical values of the delayed-fission probabilities $P_{\beta df}$ for ^{232}Pu, ^{244,248}Cf, ^{248}Fm, and ^{240}Cm. The fission barriers were calculated using the Strutinsky method (S). $P_{\beta df}$ was calculated using the nonstatistical strength functions of β^+ (EC) decay obtained in the TDA model.

Nucleus	E_A(S), MeV	E_B(S), MeV	$\hbar\omega_A$, MeV	$\hbar\omega_B$, MeV	Q_β, MeV	Exp., $P_{\beta df}$	Theor., $P_{\beta df}$
^{232}Pu	4.0	4.2	0.9	0.6	5.2	$1.3^{+4}_{-0.8}\cdot 10^{-2}$	5×10^{-2}
^{244}Cf	5.3	2.8	0.9	0.6	4.5	5×10^{-4}	4×10^{-4}
^{248}Fm	5.7	1.8	0.9	0.6	5.2	3×10^{-3}	2×10^{-3}
^{248}Cf	5.7	3.3	0.9	0.6	2.9	$<10^{-7}$	2×10^{-7}
^{240}Cm	5.2	3.7	0.9	0.6	3.9	10^{-5}	9×10^{-7}

formula.[101] In Fig. 15 we also show the fission barrier of ^{232}Pu, calculated by the method of Strutinsky shell corrections. The following parameters of the fission barrier for ^{232}Pu were used in the calculations of $P_{\beta df}$: $E_B=4.21$ MeV, $\hbar\omega_A=0.9$ MeV, $\hbar\omega_B=0.6$ MeV, and the height of the inner barrier E_A was varied. Assuming $S_\beta=$const and $P_{\beta df}=1.3\times10^{-2}$, it was found that $E_A=5.3$ MeV (i.e., the same result as in Ref. 88), which is 1–2 MeV higher than in the calculations using the Strutinsky method ($E^{th}=3.5$–4.3 MeV). However, if the $S_\beta(E)$ calculated in Ref. 32 is used and a realistic width is introduced (FWHM=1 MeV), then without any fit we find that $E_A=4.0$ MeV corresponds to $P_{\beta df}=5.0\times10^{-2}$, in agreement with experiment[87,88] and with the Strutinsky calculation of the fission barrier. Therefore, on the basis of the analysis of Ref. 32 it can be concluded that:

1. If the structure of the β strength function is taken into account in a suitable manner, the experimental data on the delayed fission of ^{232}Pu can be explained.

2. There are no grounds for stating that the fission barriers calculated using the Strutinsky method do not lead to a description of the data on delayed fission, as was done in Ref. 88.

In the actinide region, the β^+ (EC) delayed fission (βdf) has also been studied for the following processes:

$$^{240}\mathrm{Bk}\xrightarrow{\beta^+(\mathrm{EC})}{}^{240}\mathrm{Cm}\rightarrow\beta\mathrm{df},$$

$$^{244,248}\mathrm{Es}\xrightarrow{\beta^+(\mathrm{EC})}{}^{244,248}\mathrm{Cf}\rightarrow\beta\mathrm{df},$$

$$^{248}\mathrm{Md}\xrightarrow{\beta^+(\mathrm{EC})}{}^{248}\mathrm{Fm}\rightarrow\beta\mathrm{df},$$

$$^{234}\mathrm{Am}\xrightarrow{\beta^+(\mathrm{EC})}{}^{234}\mathrm{Pu}\rightarrow\beta\mathrm{df}.$$

The values of $P^{exp}_{\beta df}$ were measured in Refs. 88–91. In Fig. 15 and Table III we give the results of the calculations[5,32] of S_β, $P^{theor}_{\beta df}$, and the experimental values $P^{exp}_{\beta df}$ for a number of nuclei. In the calculation of $P_{\beta df}$ the peaks in $S_\beta(E)$ were approximated by Gaussians with FWHM=1 MeV. The ratio of the "peak" area to the "background" below the peak was chosen to be 100. These parameters for the width and background correspond to the systematics of Refs. 102 and 103. In this case the inclusion of the background models β transitions of various degrees of forbiddenness and is not very important. We see from Table III that the calculated values of $S_\beta(E)$ and $P_{\beta df}$ together with the fission barriers calculated using the Strutinsky method lead to a good description of experiment. Small discrepancies are observed where the experimental values of $P_{\beta df}$ are small (for ^{240}Cm and ^{248}Cf), but by varying the height of the fission barrier within the allowed limits (by no more than 0.5 MeV), agreement with experiment can be obtained.

The delayed fission of ^{234}Am was studied in Ref. 91. It was shown that $P_{\beta df}=(6.6\pm1.8)\times10^{-5}$. Calculations[5,32] predict that $S_\beta(E)$ has a resonance near the excitation energy $E\simeq2.5$ MeV determining the delayed-fission probability of ^{234}Am. In this case the experimental value of $P_{\beta df}$ corresponds to a ^{234}Pu fission barrier with the parameters $E_A=4.7$ MeV, $\hbar\omega_A=0.9$ MeV, $E_B=4.2$ MeV, and $\hbar\omega_B=0.6$ MeV, which agree with the values calculated by the Strutinsky method.[98,99]

It can therefore be concluded from this analysis of the experimental data on delayed fission in the actinide region that delayed fission can be correctly described only by using the nonstatistical β-transition strength function reflecting nuclear-structure effects.[5,32]

2.3. The strength functions of β^+ (EC) and β^- decays and the delayed fission of preactinide nuclei

The region of preactinide nuclei offers great possibilities for β-delayed fission. In this region there are very few experimental data on the fission probabilities and mechanism for cold nuclei, and data cannot be obtained by any of the traditional methods.[104] At present, β^+ (EC) delayed fission has been discovered experimentally in the region of neutron-deficient isotopes Hg–Pb. The observation of β^+ (EC) delayed fission near ^{180}Hg has been reported in Refs. 92, 93, and 105. The β^--delayed fission of neutron-rich isotopes of Ra is being studied.[106]

The delayed fission in the case

$$^{180}\mathrm{Tl}\xrightarrow{\beta^+(\mathrm{EC})}{}^{180}\mathrm{Hg}\xrightarrow{\text{fission}}\beta\mathrm{df}$$

has been calculated in Refs. 49 and 107. The integrated Fermi function $f(E,Z)$ for the β^+ (EC) decay of ^{180}Tl was chosen to have the form

$$f(E,Z)=f_{\beta^+}(E)+f_k(E)+f_{L_I}(E)+\ldots. \tag{43}$$

The terms correspond to the contributions from β^+ decay, K capture, and L_I capture.

For the β^+ (EC) decay of ^{180}Tl to the level with excitation energy E in ^{180}Hg, the contribution from the β^+ transi-

TABLE IV. Calculated[49,107] probabilities of β^+ (EC) delayed fission $P_{\beta df}$ for ^{180}Hg for various values of the fission-barrier height B_f and curvature $\hbar\omega$. GS means that the peaks in the strength function of β^+ (EC) decay $S_\beta(E)$ were represented as Gaussians with FWHM Δ. BW means that the peaks in S_β were represented as Breit–Wigner distributions of width Γ_{BW}. $S_\beta(E)$ was calculated using the TDA model. The experimental value[92] is $P_{\beta df}=3\times10^{-(7\pm1)}$. The first qualitative estimate[93] is $B_f\approx11$ MeV.

B_f, MeV	$\hbar\omega$, MeV	Δ, MeV	$P_{\beta df}$, GS	Γ_{BW}, MeV	$P_{\beta df}$, BW
10	1.0	1	1.4×10^{-5}	1	1.7×10^{-3}
		2	9.3×10^{-5}	2	3.7×10^{-3}
11	1.0	1	3.2×10^{-8}	1	1.1×10^{-5}
		2	2.4×10^{-7}	2	2.3×10^{-5}
12	1.0	1	5×10^{-11}	1	2×10^{-8}
		2	4×10^{-10}	2	4.1×10^{-8}

tion is only about 10% for $Q_{EC}-E=3$ MeV. It becomes comparable to the contribution of K capture at $Q_{EC}-E=5$ MeV, and two times greater than the contribution of K capture at $Q_{EC}-E=6.5$ MeV. The inclusion of L_I capture can be important at excitation energies near Q_{EC}, where the fission probabilities are especially high. The limits of the summation (integration) in (42) are different for the different terms. For β^+ decay the upper limit is $Q_{EC}-2m_ec^2$, and for K and L_I capture it is $Q_{EC}-\varepsilon_{k,L}$.

The equilibrium deformation of the ^{180}Hg nucleus was estimated before calculating $S_\beta(E)$. This deformation was calculated[49,107] by the method of Strutinsky shell corrections.[98] It turned out that the equilibrium deformation parameter in the ground state was $|\varepsilon|\leq0.1$, i.e., $S_\beta(E)$ can be calculated by assuming that ^{180}Hg is spherical.

The single-particle energies were calculated for the Woods–Saxon potential with parameters chosen as in Ref. 100. According to the estimates of Ref. 108, the value of Q_{EC} for ^{180}Tl is 10.5–11 MeV.

The calculations[49,107] performed with the Gamow–Teller residual interaction in the Tamm–Dancoff approximation show that in this case $S_\beta(E)$ can be represented as two Gaussians with widths (FWHM) of about 1 MeV and comparable intensities (1:1.9). The half-life for decay via the β^+ (EC) channel in the TDA is $T_{1/2}\approx1.8$ sec, while in the QRPA method[95] $T_{1/2}\approx0.74$ sec (for $Q_{EC}=10.9$ MeV). The experimental estimate[92] is $T_{1/2}^{exp}=0.70^{+0.12}_{-0.09}$ sec, i.e., 2.5 times smaller than the half-life of β^+ (EC) decay in the TDA and in agreement with the half-life of β^+ (EC) decay calculated[95] in the QRPA. However, the fact that α decay also contributes to the total half-life $T_{1/2}^{exp}$ must be taken into account. At present there are no experimental data on the ratio of α and β^+ (EC) decays, and theoretical estimates[95] predict roughly equal contributions of the two for ^{180}Tl. On the whole, the agreement between the theoretical and experimental values of the half-lives in calculations of this type can be considered completely satisfactory.

The delayed fission of ^{180}Hg is mainly determined by the peak in $S_\beta(E)$ at excitation energy $E^*\approx6.8$ MeV. The calculated values[49,107] of $P_{\beta df}$ for ^{180}Hg are given in Table IV. By comparing the calculated and measured values of $P_{\beta df}$, we can estimate the fission barrier of ^{180}Hg. Taking $\hbar\omega=1$ MeV, the height of the fission barrier B_f in ^{180}Hg corresponding to the experimental estimate[92] $P_{\beta df}=3\times10^{-(7\pm1)}$ will be $B_f\approx11$ MeV ($P_{\beta df}=3\times10^{-7}$), which agrees with the qualitative estimate made in Ref. 93.

The calculations of $S_\beta(E)$ using the QRPA[95] and TDA models give qualitatively similar $S_\beta(E)$ for the β^+ (EC) decay of ^{180}Tl (intense peaks in the regions 2–4 MeV and 6–8 MeV). The differences between the $S_\beta(E)$ calculated in the two models are not important for calculating $P_{\beta df}$ [because in this case $P_{\beta df}$ is determined by the peaks of $S_\beta(E)$ in the region 6–8 MeV, and it is necessary to know $S_\beta(E)$ only up to a constant), but they are important in calculating the half-lives.[5,107,109] The calculated values of $P_{\beta df}$ using $S_\beta(E)$ obtained in the QRPA give a fission-barrier height of $B_f\approx11$ MeV for ^{180}Hg, with $P_{\beta df}=8\times10^{-7}$, i.e., they agree with experiment and with the TDA calculations.

The delayed fission of a number of preactinide nuclei can be used as a test for checking the various models used to calculate $S_\beta(E)$ or the fission barriers. Studies of the β^--delayed fission[110]

$$^{232}\mathrm{Fr}\xrightarrow{\beta^-}{}^{232}\mathrm{Ra}\xrightarrow{\text{fission}}\beta\mathrm{df}$$

are very useful for this.

The experimental estimate $P_{\beta df}^{exp}<2\times10^{-6}$ for ^{232}Ra was obtained in Ref. 106. The experimental estimate for $P_{\beta df}^{exp}$ strongly contradicts the theoretical value[111] $P_{\beta df}^{theor}\approx0.3$.

The calculations of $P_{\beta df}$ are very sensitive to parameters like the total β-decay energy Q_β, the height of the fission barrier B_f, the barrier curvature $\hbar\omega_f$, and the structure of the β-decay strength function. The dependence of $P_{\beta df}$ on the barrier height and curvature $\hbar\omega_f$ is especially strong in some cases.

The calculations performed in Ref. 110 showed that for the β^- decay of ^{232}Fr the strength function $S_\beta(E)$ has a maximum at excitation energy $E^*\approx5.5$ MeV and can be approximated by a Gaussian of width FWHM≈1 MeV. If the parameter of the effective one-hump fission barrier of ^{232}Ra is chosen to be $\hbar\omega=1$ MeV, the experimental estimate $P_{\beta df}<2\times10^{-6}$ corresponds to barrier height $B_f>7.7$ MeV in ^{232}Ra. The value of Q_β was chosen as in Ref. 108 (systematics): $Q_\beta=5.7\pm0.7$ MeV.

Theoretical calculations[112] indicate that the fission barriers for ^{228}Ra and ^{232}Ra are roughly identical. Experimental data on the effective one-hump barrier of ^{228}Ra are given in Refs. 113 and 114: $B_f\approx7.8$ MeV, $\hbar\omega=0.9$ MeV; and $B_f=8.7\pm0.4$ MeV. Thus, the estimate[110] $B_f>7.7$ MeV for the barrier in ^{232}Ra is in agreement with a number of experimental and theoretical results. The value of $P_{\beta df}$ obtained in Ref. 111 is too large, which may be due to an incorrect choice of the barrier parameters.

Thus, for nuclei far from the β-stability band the calculations of $P_{\beta df}$ can give widely differing results if the energy parameters $[Q_\beta, B_f, S_\beta(E)]$ are not known sufficiently accurately. The solution of the inverse problem, i.e., estimation of the barrier parameters from the data on delayed fission, can give valuable information. However, in this case it is necessary to have information about the structure of the β-transition strength function.

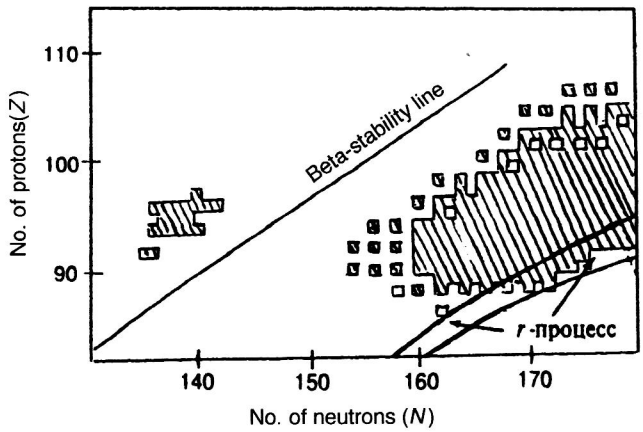

FIG. 16. A fragment of the r-process chart. The shaded region corresponds to nuclei for which delayed fission is energetically allowed.

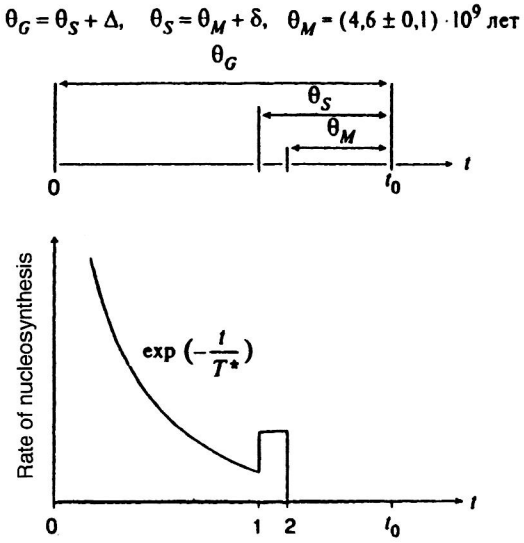

FIG. 17. Scheme of the exponential model of nucleosynthesis and the time scale. Δ is the duration of nucleosynthesis, δ is the duration of meteorite formation and hardening (2), t_0 is the present time, S is the contribution of the nucleosynthesis burst (1) before the formation of the Solar System, θ_G is the age of the Galaxy, θ_S is the age of the Solar System, and θ_M is the age of meteorites.

2.4. Delayed fission, the structure of the β-decay strength functions, and nuclear production in astrophysical processes

The relative abundances of nuclei of various elements in our region of the Universe display a number of regularities which can be associated with the properties of the astrophysical processes in which these elements are synthesized.[111,115–119]

Heavy nuclei, i.e., nuclei heavier than iron, are apparently formed as a result of neutron capture followed by β^- decay.[1] If the neutron capture is faster than the β decay, neutron-rich nuclei are produced. The significant abundance of such nuclei in the Solar System indicates that fast neutron capture (the r-process) plays an important role in matter evolution in the Universe.[1] After the r-process, which can occur, for example, in a supernova burst,[120,121] the synthesized nuclei decay to the β-stability line. The number of nuclei of a given element near the stability line depends on the competition of several processes: β^- decay, delayed fission, and the emission of delayed neutrons and γ rays.[121,122]

To check the various cosmological models, it is important to estimate the time scales of the evolution of the Universe. Times of this type can be estimated by using the ratios of concentrations of particular isotope-chronometric pairs:[123] ^{238}U/^{232}Th, ^{235}U/^{238}U, ^{244}Pu/^{232}Th, and ^{247}Cm/^{232}Th. The effect of delayed fission can be very important in the production of chronometric pairs; it has been estimated in Ref. 124. However, in the studies listed above the effect of the structure of the β-transition strength function on nuclear production in astrophysical processes, was not taken into account. The need to include the structure of $S_\beta(E)$ in analyzing the r-process and in chronometric-pair production has been pointed out in Refs. 5, 14, and 31. The structure of $S_\beta(E)$ was analyzed in Refs. 5 and 125 for several nuclei participating in the r-process, using the shell model including the Gamow–Teller residual interaction. The chart of the r-process is shown in Fig. 16 (Ref. 126). It turned out that for nuclei with $A=250-266$ and $N=165-175$ (parent nuclei),[5,125] the excitation energy E_i of the peak in $S_\beta(E)$ determining delayed fission can be written as follows for Gamow–Teller β^- transitions:

$$E_i(\text{MeV}) \simeq -0.15(N-160)+0.46(Z-8)-B, \qquad (44)$$

where $B=0.3-3$ MeV. This dependence can be extrapolated up to $N\simeq 200$. This behavior of $S_\beta(E)$ agrees quite well with the later calculations.[68] When $S_\beta(E)$ is calculated for nuclei participating in the r-process, it is necessary to make a number of extrapolations to nuclei which are rather far from the stability band. Although the estimates of $S_\beta(E)$ are quite sensitive to the choice of extrapolation, such calculations can indicate whether or not there is structure in $S_\beta(E)$ and whether or not it should be taken into account in analyzing nuclear production in astrophysical processes.[5,68,125]

Let us qualitatively discuss the effect of structure in $S_\beta(E)$ on the formation of the cosmo-chronometric pairs ^{238}U/^{232}Th, ^{235}U/^{238}U, ^{244}Pu/^{232}Th, and ^{247}Cm/^{232}Th. The exponential model of nucleosynthesis and its time scale[119] are shown schematically in Fig. 17. The time evolution in nucleosynthesis is determined by the following parameters: the duration of nucleosynthesis Δ, the contribution S of a burst of nucleosynthesis to nuclear production before the formation of the Solar System, the nucleosynthesis exponent parameter T^*, the duration of meteorite production δ, and the present time t_0. The age of meteorites is determined in independent experiments and is[119] $\theta_M=(4.6\pm0.1)\times10^9$ yr. Information on the age of a chronometric pair is contained in the parameter $R(i,j)=(P_i/P_j)/(N_i/N_j)$ and the half-lives of the nuclei forming the pair. Here P_i/P_j is the ratio of the number of nuclei after the series of β decays following the r-process at time $t=\Delta+\delta$ (Fig. 17), and N_i/N_j is the ratio at the present time. By measuring N_i/N_j, the half-lives, and the age of meteorites, and calculating P_i/P_j and R_i/R_j, we can estimate the time parameters of astrophysical processes by using various models of the r-process.

The yield $P(\Delta+\delta)$ of nuclide i at the time when the meteorite material hardens is given by[119]

TABLE V. Ratios of cosmo-chronometer production rates in the r-process: (*) neglecting delayed fission; (**) including delayed fission, but with $S_\beta(E)\simeq\rho(E)$; (***) including delayed fission and the structure in the β strength function $S_\beta(E)$.

Isotopes	$a_i(0)/a_j(0)$ (*)	$a_i(0)/a_j(0)$ (**)	$a_i(0)/a_j(0)$ (***)
^{244}Pu/^{232}Th	0.47 ± 0.1	0.31	0.12
^{235}U/^{238}U	1.5 ± 0.5	0.89	1.24
^{232}Th/^{238}U	$1.9^{+0.2}_{-0.3}$	1.7	1.4
^{247}Cm/^{232}Th	0.34	0.15	0.21

$$P_i(\Delta+\delta)\simeq a_i(0)\exp(-\lambda_i\delta)\left[\frac{1-S}{1-\lambda_i T^*}\times\frac{\exp(-\lambda_i\Delta)-\exp(-\Delta/T^*)}{1-\exp(\Delta/T^*)}+S\right]$$
$$=a_i(0)\varphi_i(\Delta,S,T^*,\delta,\lambda_i), \quad (45)$$

where $a_i(0)$ is the rate of production of nuclide i at the start of nucleosynthesis and λ_i is the decay constant of nuclide i. To evaluate the four unknowns (Δ, S, T^*, and δ), it is necessary to have at least four independent quantities: the yield ratios

$$\frac{P_i(\Delta+\delta)}{P_j(\Delta+\delta)}=\frac{a_i(0)}{a_j(0)}\cdot\frac{\varphi_i(\Delta,S,T^*,\delta,\lambda_i)}{\varphi_j(\Delta,S,T^*,\delta,\lambda_j)} \quad (46)$$

and the four ratios of nuclide production rates $a_i(0)/a_j(0)$ calculated by using various models of nucleosynthesis. The inclusion of the structure of $S_\beta(E)$ is important in calculating the ratios $a_i(0)/a_j(0)$.

In Table V we give the values of $a_i(0)/a_j(0)$ for several cosmo-chronometers obtained by neglecting delayed fission[127] (*), including delayed fission[126] but with $S_\beta(E)\simeq\rho(E)$ (**), and including delayed fission and the structure[111] of $S_\beta(E)$ (***). The important role of delayed fission and the structure of $S_\beta(E)$ is obvious from the data in Table V. However, it should be borne in mind that the calculations of the delayed-fission probability for many of the nuclei produced in the r-process are rather unreliable,[71] and so some of the conclusions are only qualitative. The parameter $R(i,j)$ is not model-independent, because the ratio P_i/P_j depends on the dynamics of the r-process, and also on the subsequent neutron irradiation,[122] and by using cosmo-chronometric pairs it is possible to obtain only model estimates of the time parameters of nucleosynthesis.

The first calculations of the ratios $a_i(0)/a_j(0)$ taking into account delayed fission were made in Ref. 122. It was shown that near $A\simeq145$ the probability of β-delayed fission is significant, $P\simeq0.5$, which tends to decrease the production of ^{235}U and ^{244}Pu, and so when delayed fission is included, $a_i(0)/a_j(0)$ for ^{244}Pu/^{232}Th and ^{235}U/^{238}U is significantly decreased. Meanwhile, $a_i(0)/a_j(0)$ for ^{232}Th/^{238}U varies rather less than the data of Ref. 127. However, $S_\beta(E)\simeq\rho(E)$ was used in Ref. 122, and in this case the fraction of delayed fission near $A\simeq244$ is determined by the fraction of β^- transitions occurring in an energy interval about 1 MeV below the ground state of the parent nucleus.[5] If we take the $S_\beta(E)$ calculated in Refs. 5 and 125 with peak width FWHM=1 MeV, the fraction of β^- transitions falling in this interval is smaller than for $S_\beta(E)\simeq\rho(E)$. Then the ratios $a_i(0)/a_j(0)$ for cosmo-chronometers must be increased in relation to the data of Ref. 122, but remain smaller than in Ref. 127. This conclusion has been confirmed in Ref. 111. The following estimates of the nucleosynthesis time parameters were obtained in that study:[111] $\Delta\simeq16\times10^9$ yr and the age of the Galaxy $\theta_G=(\Delta+\delta+4.6\times10^9\text{ yr})=20.8\times10^9$ yr. These values of Δ and θ_G exceed the values obtained earlier,[128] which leads to rather interesting conclusions. However, their discussion lies outside the scope of this review.

Thus, all the data discussed above unambiguously indicate that delayed nuclear fission and related processes can be analyzed correctly only by using the nonstatistical strength function of β^- and β^+ (EC) decays taking into account nuclear-structure effects.

3. NONSTATISTICAL EFFECTS IN (p,γ) AND $(p,p'\gamma)$ NUCLEAR REACTIONS WITH THE EXCITATION AND DECAY OF NONANALOG RESONANCES

3.1. Studies of the resonance structure in reactions involving low-energy protons

Studies of nuclear structure in reactions involving protons are important in the development of our ideas about nuclear structure. Here the study of the properties and structure of various resonances is particularly important. The region of excitation energies where clearly expressed resonances can be observed in reactions induced by protons reaches 10–12 MeV in nuclei with $A\simeq60$ and 15–17 MeV in light nuclei, where the level density is low. As a rule, only analog resonances are observed in nuclei with $A>70$ in the cross sections for reactions involving protons. Analog resonances are excited in proton elastic and inelastic scattering on nuclei up to bismuth, and their widths range from a fraction of a keV to several keV.[6] An analog resonance is a structure like a giant resonance, formed owing to the distribution of the strength of a "simple" excitation over the levels of the compound nucleus, where the isospin of the analog is one unit larger than that of the states of the compound nucleus. The special nature of an analog resonance and the related nonstatistical effects are well known[6,129] and are due to the isospin symmetry of the nuclear forces. A large number of other, nonanalog, resonances are observed in the excitation functions of the $(p,p'\gamma)$ and (p,γ) reactions.[4,11,13] There are two possible interpretations of nonanalog resonances. One is that they are statistical resonances of a compound nucleus, and the other is that they are structures like the giant resonance, associated with the distribution of simple excitations (for example, excitations like the GT resonance or its satellites) over the levels of the compound nucleus. In the second case the physical interpretation of the experiments should differ from the statistical interpretation. In the present section we shall analyze the manifestation of

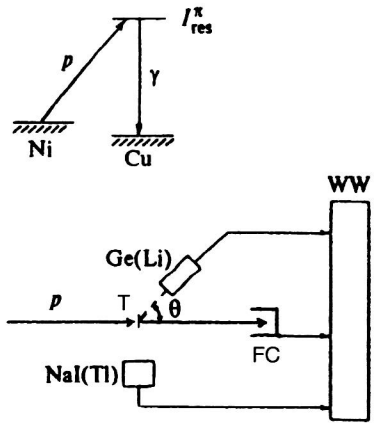

FIG. 18. Experimental setup for studying resonance excitation and decay in the (p,γ) reaction: p is the proton beam, T is the target, FC is a Faraday cylinder, Ge(Li) is a germanium–lithium detector placed at angle θ relative to the proton beam, NaI(Tl) is a scintillation detector, and WW is the data storage and analysis system.

nonstatistical effects in (p,γ) and $(p,p'\gamma)$ nuclear reactions in the excitation and decay of the nonanalog resonances of a compound nucleus.

3.2. The experimental technique

A significant amount of experimental data on (p,γ) reactions has been obtained[11,13,15] by bombarding Ni targets with low-energy protons. The experiments were performed at the EG-5 electrostatic generator. The targets of isotopes ^{58,60,62}Ni (95% enrichment) were 20–40 μg/cm^2 thick. The energy of the accelerated protons could be varied when seeking resonances, and its maximum value could reach 5 MeV. The currents reached 10 μA. The experimental technique is described in detail in Refs. 11, 13, and 30. This technique has been used to find nonstatistical correlations of the reduced γ-decay widths $[B(E2)$ and $B(M1)]$ of nonanalog resonances,[12,130] to reveal and study nonstatistical effects in the γ-ray angular distributions,[15,131] and to estimate the fraction of the nonstatistical component in the wave functions of nonanalog resonances.[132] The experimental setup and the (p,γ) reaction are shown schematically in Fig. 18. Resonances in the excitation function were sought by using a γ spectrometer with a detector based on a NaI(Tl) crystal of area 100×100 mm. The spectrometer operated in the integrated- counting mode. The discrimination threshold was chosen so that the energies of the recorded γ rays amounted to half of the excitation energy $E^*/2$ in the given nucleus. This discrimination threshold eliminated background γ lines with energy less than $E^*/2$, while a significant fraction of the γ rays from resonance decay were recorded. If the resonance γ decay occurred to nuclear levels with excitation energy less than $E^*/2$, the spectrometer recorded these transitions $(E_\gamma > E^*/2)$. In resonance decay to levels with energy greater than $E^*/2$, γ transitions from these levels to the ground state and a number of low-lying states $(E_\gamma > E^*/2)$ were recorded.

The thickness of the target was chosen so that the energy losses in it were of the order of the accelerator resolution and smaller than the distance between resonances. For nuclei with $A \simeq 60$ and $E_p < 5$ MeV at resolution $\Delta E_p \simeq 1-2$ keV, it is convenient to use a target of thickness 10–20 μg/cm^2. After a resonance was found, the γ spectra of its decay were measured by a Ge(Li) detector of volume 40 cm^3 and energy resolution 7–8 keV for a γ energy of 7 MeV.

The γ spectra were measured at the angles 0°, 30°, 60°, and 90° to the incident beam direction for each resonance studied. The proton beam intensity, the integrated intensity of γ rays recorded by the NaI(Tl) crystal, and also the intensity of γ lines recorded by the second Ge(Li) detector at 135° were determined when measuring the angular distributions, which allowed reliable normalization of the γ spectra obtained at different angles.

The energy calibration of the γ rays in the region up to 2.6 MeV was done using many internal reference points. At high excitation energies, convenient reference points were the photopeak and the peaks corresponding to single and double emission of the γ transition of energy 6.129 MeV, arising in the reaction ^{19}F$(p,\alpha)^{16}$O.

The angular distributions of the γ rays are represented as an expansion in Legendre polynomials:

$$W(\theta) = \sum_k A_k P_k(\cos\theta), \tag{47}$$

where θ is the angle between the beam direction and the γ detector.

For (p,γ) reactions and targets with zero nuclear spin, in the excitation of an isolated resonance with a definite spin the coefficients of the expansion (47) depend only on the resonance spin (I_{res}), the spin of the final state (I_f), and the mixture of multipole orders:

$$\delta = \frac{\langle I_f \| E2 \| I_{\text{res}} \rangle}{\langle I_f \| M1 \| I_{\text{res}} \rangle}, \tag{48}$$

where $\langle I_f \| O_\gamma \| I_\gamma \rangle$ is the reduced matrix element of the $E2$ or $M1$ γ transition.[132] Expressions relating A_k to I_{res}, I_f, and δ are given in Ref. 15.

The experimental angular distributions for γ transitions from the studied resonance, whose spin is unknown, are compared with the theoretical distributions for various values of δ and I_{res}. The spins of the final states (I_f, low-lying levels) are known from other experiments. Then the function

$$\chi^2(\delta) = \sum_{i=1}^{N} \frac{(Y_i - W_i)^2}{\sigma_i^2} \tag{49}$$

is constructed[11,21] for various values of I_{res}, where Y_i is the experimental value of the γ-transition intensity at angle θ_i, W_i is the theoretical value of the intensity, and σ_i is the standard deviation of Y_i. The values of I_{res} and δ are determined from the χ^2 minimum. An example of this analysis taken from Ref. 13 is shown in Fig. 19. The minimum value of χ^2 (Fig. 19b) for the angular distribution of the γ transition in Fig. 19a corresponds to the best choice of the resonance spin I_{res} and multipole mixture δ.

The angular distribution for a single γ transition sometimes does not allow the unique determination of the resonance spin. A combined analysis of the angular distributions

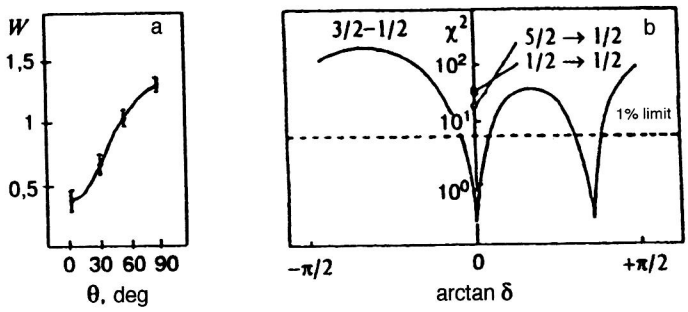

FIG. 19. Analysis of the ^{60}Ni$(p,\gamma)^{61}$Cu reaction for the resonance at $E_p = 2442$ keV (E_p is the incident-proton energy, and E^* is the excitation energy of the ^{61}Cu nucleus). The angular distribution (a) and the χ^2 analysis (b) are given for the γ transition from the resonance at $E^* = 7193$ keV ($E_p = 2442$ keV) to the level at 475 keV in ^{61}Cu. The dependence of χ^2 on the arctangent of the multipole mixture δ for the $\frac{3}{2}\rightarrow\frac{1}{2}$ γ transition and the minimum of χ^2 for the $\frac{5}{2}\rightarrow\frac{1}{2}$ and $\frac{1}{2}\rightarrow\frac{1}{2}$ γ transitions are given.

of several transitions from a given resonance can significantly simplify the determination of the resonance spin. The quantity δ is a quadratic function of the coefficient A_2, and so solution of this equation gives two values of δ. The χ^2 minimum is also reached for two values of δ. As a rule, one of these two values is small and corresponds to dominant contribution of the $M1$ multipole order to the transition intensity. The second value is large and corresponds to dominant contribution of the $E2$ transition. According to the systematics[30,133] for γ transitions in nuclei of the $f-p$ shells, strong $M1$ transitions with $E2$ admixture only rarely exceeding 10% are typical. Therefore, as a rule, large values of δ can be discarded, because they lead to values of $B(E2)$ which are too large. However, in general it is impossible to recommend any particular value of δ in such experiments. It is therefore generally more convenient to analyze nonstatistical effects by using the coefficients A_2 directly.[15]

Let us consider the determination of the spins and multipole mixtures for the reaction ^{60}Ni$(p,\gamma)^{61}$Cu. The properties of the resonances in this reaction at proton energy $E_p = 1920-2460$ keV were studied in Ref. 13. In Fig. 19 we give the angular distribution (Fig. 19a) and the χ^2 analysis (Fig. 19b) for the γ transition from the resonance at $E_p = 2442$ keV to the 475-keV level in ^{61}Cu. The spin of the final state with $E^* = 475$ keV is known: $I_f = \frac{1}{2}^-$ (Ref. 62). The χ^2 analysis of the resonance with $E_p = 2442$ keV and excitation energy $E^* = 7193$ keV allows the unique assignment of the spin $I_{res} = \frac{3}{2}$, because the minimum values of χ^2 for $I_{res} = \frac{1}{2}$ or $\frac{5}{2}$ (shown by the * in Fig. 19b) significantly exceed the χ^2 minimum for $I_{res} = \frac{3}{2}$. These resonances are assigned negative parity. The parity determination is based on the fact that in this region there must be resonances with a strong single-particle $P_{3/2}$ component ($l=1$). Resonances with positive parity ($l=2$) must have a lower excitation cross section, owing to the stronger centrifugal barrier. In addition, in this range of excitation energies no mixed transitions of the $E1+M2$ type have been discovered for the nuclei in question,[1,29] and so nonzero values of δ indicate the presence of an $M1+E2$ mixture, which in this case is typical for resonances of negative parity.

3.3. Nonstatistical effects in the angular distributions in (p,γ) reactions

For a target of even–even nuclei, the angular distribution of the γ radiation in the (p,γ) reaction for a resonance i and the transition $I_{res} = \frac{3}{2} \xrightarrow{\gamma} I_f = \frac{3}{2}$ is written as[15]

$$W_i(\theta) = \sum_k A_k(i) P_k(\cos\theta),$$

$$A_2(i) = \frac{0.4 - 1.55\delta_i}{1+\delta^2}, \quad A_4 = 0. \tag{50}$$

The distributions of the matrix elements or the multipole mixtures δ are calculated in various models. The coefficients $A_2(i)$ are measured experimentally, and, as a rule, the values of δ are extracted using a number of assumptions. It is therefore interesting to obtain expressions directly for the distributions of the coefficients A_2 and to compare them with experiment. This has been done in Refs. 9, 15, and 131.

In the statistical model the matrix elements of γ transitions follow a normal distribution with zero average and standard deviation σ. In this case the probability density of δ for the resonance in question is described by the Cauchy distribution:[11]

$$P(\delta) = \frac{a}{\pi(a^2+\delta^2)}, \tag{51}$$

where $a = \sigma(E2)/\sigma(M1)$. It follows from (51) that the average is $\langle\delta\rangle = 0$ and that the distribution of δ is symmetric about $\delta = 0$.

As was shown in Ref. 15, the probability density $P(A_2)$ for the coefficients A_2 is related to $P(\delta)$ in a model-independent way:

$$P(A_2) = P[\delta_1(A_2)]\left|\frac{d\delta_1}{dA_2}\right| + P[\delta_2(A_2)]\left|\frac{d\delta_2}{dA_2}\right|, \tag{52}$$

where $\delta_1(A_2)$ and $\delta_2(A_2)$ are the two solutions of the quadratic equation relating A_2 and δ. Then for the (p,γ) reaction $I_{res} \xrightarrow{\gamma} I_f = \frac{3}{2}$ we have[15]

$$\delta_1(A_2) = \frac{-0.775 + \sqrt{0.6 - A_2(A_2 - 0.4)}}{A_2},$$

$$\delta_2(A_2) = \frac{-0.775 - \sqrt{0.6 - A_2(A_2 - 0.4)}}{A_2}. \tag{53}$$

Substituting (51) and (53) into (52), we obtain the expression for the density distribution of the coefficients A_2 in the statistical model.[15] It is simplest to write $P(A_2)$ in the statistical model for $a = \sigma(E2)/\sigma(E1) = 1$:

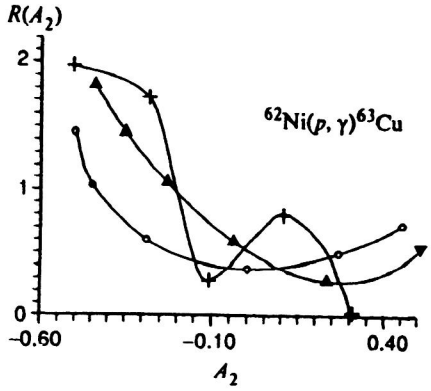

FIG. 20. Calculated and experimental values of the distributions $P(A_2)$ of coefficients A_2 for the γ decay of nonanalog resonances with $I^\pi=\frac{3}{2}^-$ to the ground state of the ^{63}Cu nucleus: ○ is for the statistical model, + is from experiment, and ▲ is for the nonstatistical model.

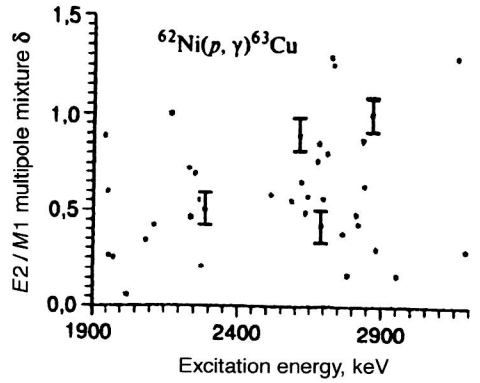

FIG. 21. Dependence of the multipole mixture δ on the incident-proton energy for nonanalog resonances with $I^\pi=\frac{3}{2}^-$ in ^{63}Cu. The excitation energies of resonances in ^{63}Cu ranged from 8040 to 9250 keV. The average value of δ is $\langle\delta\rangle=(0.6\pm0.1)$, while the statistical model gives $\langle\delta\rangle=0$.

$$P(A_2)=\frac{1}{2\pi\sqrt{0.6-A_2(A_2-0.4)}},$$

$$\int_{0.6}^{1}P(A_2)dA_2=1. \qquad (54)$$

When comparing with experiment, the parameter a is varied to obtain the best description of the experimental data.[15]

In the statistical model, decays via different spin channels are uncorrelated. The distribution taking into account nonstatistical correlations of $E2$ and $M1\,\gamma$ transitions is given in Ref. 15. In the case of the (p,γ) reaction, $E2$ and $M1\,\gamma$ decay, and constant correlation coefficient for the matrix elements of $E2$ and $M1\,\gamma$ transitions, the distribution is

$$P(\varphi)=\frac{1}{\pi}\frac{\sqrt{|a^2-\langle\delta\rangle^2|}}{a^2\cos^2\varphi+\sin^2\varphi-\langle\delta\rangle\sin 2\varphi},$$

$$\varphi=\arctan(\delta), \qquad (55)$$

where $\langle\delta\rangle$ is the average value of δ. The known analytic expressions (50) and (53) relating δ and the coefficients A_2 can be easily used to calculate the distributions $P(A_k)$. Naturally, for $\langle\delta\rangle\to0$ we obtain the corresponding expressions of the statistical model.

The angular distributions for γ decay to the $I_f^\pi=\frac{3}{2}^-$ ground states have been studied in Refs. 11–13, 15, and 135 for 19, 25, and 37 nonanalog resonances with spin and parity $I_{\rm res}^\pi=\frac{3}{2}^-$ in the nuclei ^{59,61,63}Cu. The excitation-energy range was 5.3–7 MeV for ^{59}Cu, 6–7 MeV for ^{61}Cu, and 8–9.5 MeV for ^{63}Cu.

Data on the characteristics of resonances with $I^\pi=\frac{3}{2}^-$ are given in Refs. 11, 13, and 15. These data have been used[15] to obtain the experimental probability densities $P(A_2)$. The results of the analysis of $P(A_2)$ for ^{62}Ni$(p,\gamma)^{63}$Cu are shown in Fig. 20. In Fig. 21 we give the dependence of the multipole mixture δ for γ transitions on the energy of resonances in ^{63}Cu. The dependence $\delta(E_p)$ in the reactions ^{58,60}Ni$(p,\gamma)^{59,61}$Cu has the same behavior as in the reaction ^{62}Ni$(p,\gamma)^{63}$Cu, and the distributions $P(A_2)$ also do not correspond to the statistical model.[15] Experimental data on the average values of δ have been obtained in Refs. 15 and 132:

$$\langle\delta\rangle=(0.5\pm0.1)\ \text{ in }\ ^{59}\text{Cu},$$

$$\langle\delta\rangle=(0.7\pm0.1)\ \text{ in }\ ^{61}\text{Cu},$$

$$\langle\delta\rangle=(0.6\pm0.1)\ \text{ in }\ ^{63}\text{Cu}. \qquad (56)$$

The statistical model gives the value $\langle\delta\rangle=0$, which does not agree with experiment.

In Fig. 20 we show both the experimental probability densities $P(A_2)$ and the theoretical values[15] obtained from the statistical model [$\langle\delta\rangle=0$; Eq. (54)] and the model of Ref. 15, which includes nonstatistical correlations of $E2$ and $M1\,\gamma$ transitions (55). The parameter $\langle\delta\rangle$ was chosen from the experimental estimate (56), $\langle\delta\rangle=0.5$–0.7, and the parameter a in (55) was varied to obtain the best agreement with experiment. Comparison of the calculations and experiment leads the following conclusions:[15]

1. The statistical model does not describe the experimental data on the distribution density of A_2 in the reactions ^{58,60,62}Ni$(p,\gamma)^{59,61,63}$Cu.

2. The distributions $P(A_2)$ including correlations of $E2$ and $M1\,\gamma$ transitions give a better description of the experimental data in the reactions ^{58,62}Ni$(p,\gamma)^{59,63}$Cu. In both cases (for the statistical model and the model including $E2$ and $M1$ correlations), for the reaction ^{60}Ni$(p,\gamma)^{62}$Cu the theoretical estimates of $P(A_2)$ disagree significantly with experiment.

3. To obtain the best agreement between theory and experiment, it must be assumed that the parameter a in (55) depends on the resonance energy, which corresponds to taking into account the details of the nuclear excitation-energy distribution of the simple configurations in the resonance wave functions.

The values of the components in the resonance wave functions due to nonstatistical effects (the "simple" or nonstatistical components) were estimated[132] on the basis of analysis of the angular distributions in (p,γ) reactions. The resonance wave function was written as

$$\Psi_i=\sum_j C_{ij}\varphi_j+C_{n_i}\varphi_n, \tag{57}$$

where C_{n_i} is the admixture of the nonstatistical ("simple") component φ_n for the resonance i and $\Sigma_j C_{ij}\varphi_j$ is the statistical part of the wave function of the resonance i. The C_{ij} are random numbers, and

$$\sum_j |C_{ij}|^2+|C_{n_i}|^2=1. \tag{58}$$

The average values of the coefficients $\langle|C_{n_i}|^2\rangle$ for the ^{58,60,62}Ni$(p,\gamma)^{59,61,63}$Cu reactions are 20–50%, i.e., the resonances excited in the (p,γ) reaction cannot be described by the purely statistical model. A similar conclusion was reached in Ref. 30 on the basis of different considerations. The linear correlation coefficient of the γ widths of transitions from components of the fine structure of the $p_{3/2}$ analog in ^{61}Cu to the ground state and to the excited $p_{1/2}$ and $f_{5/2}$ states of this nucleus was studied in Ref. 30. In γ decay to the ground state, the γ widths are determined by the certainly nonstatistical component of the analog with large isospin $(T_>)$. In γ decay to the $p_{1/2}$ and $f_{5/2}$ states, the γ widths are determined by the assumed statistical, admixed component with smaller isospin $(T_<)$. If the $T_<$ component is statistical in nature, there should be no correlations between the γ widths. However, analysis of the experimental data[30] revealed the presence of correlations between the γ widths, which implies that the states $T_<$ do not have the complex nature characteristic of the statistical model.

3.4. Correlations of $B(E2)$ and $B(M1)$ in the ^{58,60,62}Ni$(p,\gamma)^{59,61,63}$Cu reactions

In the statistical model there are no correlations between the partial widths for decays via different channels.[136] Nonstatistical correlations of the reduced probabilities of $E2$ and $M1$ γ decays of nonanalog resonances in ^{58,60,62}Ni$(p,\gamma)^{59,61,63}$Cu reactions were discovered in Refs. 9, 12, and 131.

The angular distribution of the γ rays in γ transitions from various resonances with fixed spin and parity $J_f^\pi=\frac{3}{2}^-$ to the ground state of the Cu nucleus $(J_f^\pi=\frac{3}{2}^-)$ in the reaction Ni(p,γ)Cu were studied experimentally, along with the quantities (Refs. 9, 12, 130, and 131)

$$x_i=\frac{I_{\gamma_i}\delta_i^2 k_p^2}{(1+\delta^2)E_{\gamma_i}^5 W_i(\theta)\varepsilon_\gamma(i)},$$

$$y_i=\frac{I_{\gamma_i}k_p^2}{(1+\delta_i^2)E_{\gamma_i}^3 W_i(\theta)\varepsilon_\gamma(i)}, \tag{59}$$

where I_{γ_i} and E_{γ_i} are the intensity and energy of the γ transition, k_p is the proton wave vector, and $\varepsilon_\gamma(i)$ is the efficiency of detecting γ rays of energy E_{γ_i}. Then the correlation coefficient $\rho(x,y)$ is calculated:

$$\rho(x,y)=\frac{\Sigma_i(x_i-\langle x\rangle)(y_i-\langle y\rangle)}{[\Sigma_i(x_i-\langle x\rangle)^2\Sigma_i(y_i-\langle y\rangle)^2]^{1/2}}\kappa, \tag{60}$$

where κ is a correction associated with the errors in determining x_i and y_i (Refs. 30 and 137):

$$\kappa\approx\left\{1-\frac{1}{2}\left[\frac{\Sigma_i(\Delta x_i)^2}{\Sigma_i(x_i-\langle x\rangle)^2}+\frac{\Sigma_i(\Delta y_i)^2}{\Sigma_i(y_i-\langle y\rangle)^2}\right]\right\}. \tag{61}$$

If we work with energy resolution of the incident proton beam $\Delta E_p\gg\Gamma$ and $\Gamma_\gamma\ll\Gamma_p$, then[130]

$$\rho(x,y)=\rho(B(E2),B(M1)), \tag{62}$$

where Γ is the total resonance width, Γ_p is the width in the entrance channel, and $B(E2)$ and $B(M1)$ are the reduced probabilities of $E2$ and $M1\,\gamma$ decay. It is the situation described above which was realized in the experiments of Refs. 11, 13, and 130. The protons were accelerated by the EG-5 electrostatic generator. The proton energy resolution was 2–3 keV, which allowed resonances to be separated from each other. The value of Γ_γ is of order 10^{-2} eV, and $\Gamma_p\simeq 10-100$ eV (Refs. 6, 12, and 30), i.e., the situation in which (62) holds is realized. For determining the correlation coefficient $\rho(B(E2),B(M1))$, the values of $B(E2)$ and $B(M1)$ can be known up to a constant, because according to (60) this constant cancels. This made it possible[12,130] to use the relative intensities of the γ transitions to calculate ρ in (p,γ) reactions, which leads to a smaller error in the result than in absolute methods. In fact, in the traditional method of determining the absolute values of Γ_γ using a "thick" $(\simeq 500\,\mu g/cm^2)$ target,[6,30] it is necessary to know the isotopic composition of the target, the stopping power of the target matter, the proton charge incident on the target, and the efficiency ε_γ of the γ detector. In experiments using a "thin" $(\simeq 20\,\mu g/cm^2)$ target, it is necessary to know only the relative efficiencies ε_γ, the total proton charge, and the γ intensity. The relative efficiency ε_γ was determined from the known[21,130] balance of the intensities of γ transitions of resonances studied by many authors (the resonances corresponding to incident-proton energy $E_p=1424$ keV in ^{59}Cu, $E_p=1599$ keV in ^{61}Cu, and $E_p=2659$ keV in ^{63}Cu). To monitor the depletion of the target in the course of the experiment, the γ intensities were measured for reference resonances.[12,130]

The value of $\rho(B(E2),B(M1))$ for γ decay to the ground state of ^{63}Cu of $n=37$ nonanalog resonances with $J^\pi=\frac{3}{2}^-$ and excitation energy E from 8.04 to 9.25 MeV was determined in the reaction ^{62}Ni$(p,\gamma)^{63}$Cu. It was found that[12,130]

$$\rho(B(E2),B(M1))=0.6\pm 0.1.$$

For the reaction ^{60}Ni$(p,\gamma)^{61}$Cu, $n=25$ nonanalog resonances with $J^\pi=\frac{3}{2}^-$ and E_i ranging from 6.2 to 7.2 MeV were studied. It turned out that for γ decay to the ground state of ^{61}Cu,

$$\rho(B(E2),B(M1))=0.6\pm 0.1.$$

For the reaction ^{58}Ni$(p,\gamma)^{59}$Cu, $n=19$ nonanalog resonances with $J^\pi=\frac{3}{2}^-$ and excitation energy ranging from 5.5 to 6.8 MeV were studied. For γ decay to the ground state of ^{59}Cu it was found that

$$\rho(B(E2),B(M1))=0.7\pm 0.1.$$

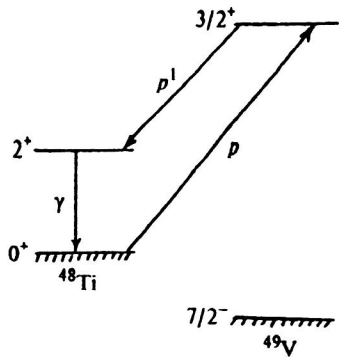

FIG. 22. Scheme of proton inelastic scattering.

Thus, these experiments and their analysis[12,130] established the presence of correlations between the reduced probabilities for $E2$ and $M1\,\gamma$ transitions in the γ decay of nonanalog resonances with $J^\pi=\frac{3}{2}^-$ in $^{58,60,62}\mathrm{Ni}(p,\gamma)^{59,61,63}\mathrm{Cu}$ reactions, which indicates that the studied resonances are nonstatistical in nature.

The set of experimental data on the angular distributions in the γ decay of nonanalog resonances with $J^\pi=\frac{3}{2}^-$ in the $^{58,60,62}\mathrm{Ni}(p,\gamma)^{59,61,63}\mathrm{Cu}$ reactions and their analysis shows that the nonanalog resonances studied in Refs. 11–13, 15, 130–132 are nonstatistical in nature.

3.5. Nonstatistical effects in $(p,p'\gamma)$ reactions

There have been many studies devoted to $(p,p'\gamma)$ reactions with resonance production in the compound nucleus (Refs. 4, 10, 134, 138, and 139). The reaction scheme is shown in Fig. 22. The proton and γ angular distributions, the $p'-\gamma$ angular correlations, and the decay widths of the resonances of the compound nucleus are studied experimentally. Nuclei with $J^\pi=0^+$ are used as the target. Resonance decay can occur via various spin channels. For example, for the decay of $J^\pi=\frac{3}{2}^+$ resonances with excitation of the $J^\pi=2^+$ state (Fig. 22), the proton can carry off angular momentum $l=0$ or $l=2$ and the channel spin can be $\frac{1}{2}$, $\frac{3}{2}$, or $\frac{5}{2}$. The probability for resonance decay with the emission of a particle i is characterized by the reduced width γ_i^2, which is related to the partial width Γ_i corresponding to resonance decay with the emission of particle i and the transmissivity P_i of the particle-emission barrier as

$$\gamma_i^2=\Gamma_i/P_i. \tag{63}$$

The ratio of the amplitudes for decays via different spin channels is

$$\delta_s=\gamma_s/\gamma_{s'}. \tag{64}$$

In the experiments of Refs. 4, 10, 134, 138, and 139, the behavior of the reduced widths follows a Porter–Thomas distribution, i.e., it is consistent with the statistical model. But from the viewpoint of the statistical model, there are no correlations between the widths and amplitudes for decays via different spin channels, and positive and negative values of δ_s are equally likely. In Refs. 4, 10, 134, 138, and 139, three types of nonstatistical effect were found: correlations of the reduced widths and reduced amplitudes in decays via different spin channels, and also δ_s distributions inconsistent with the statistical model. Various combinations of these nonstatistical effects can be found for a given nucleus at different resonance excitation energies.

TABLE VI. Linear correlation coefficients of the reduced widths and amplitudes for the decay of $J^\pi=\frac{3}{2}^+$ nonanalog proton resonances via various spin channels in the reaction $^{48}\mathrm{Ti}(p,p'\gamma)$ for incident-proton energies in the range $E_p=2.42$–3.08 MeV. The values of the correlation coefficients ρ_{ij} for the reduced widths are given in the rows of the table above the diagonal. Below the diagonal (positions ji) are the levels of statistical significance of the ρ_{ij}. The correlation coefficients of the reduced amplitudes are listed under the table. γ_p^2 are the reduced elastic-scattering widths, and γ_{ab}^2 are the reduced inelastic-scattering widths, where a is the orbital angular momentum of the inelastically scattered proton and $b=2S$; S is the total spin of the exit channel.

Widths	γ_p^2	γ_{03}^2	γ_{23}^2	γ_{25}^2
γ_p^2	1	0.02	−0.05	0.00
γ_{03}^2	8%	1	0.43	0.85
γ_{23}^2	19%	98%	1	0.15
γ_{25}^2	1%	>99.9%	56%	1

$\rho(\gamma_{03}\gamma_{23})=0.84$; $\rho(\gamma_{23}\gamma_{25})=-0.65$; $\rho(\gamma_{03}\gamma_{25})=-0.57$.

As a typical example, let us present the data[138,139] on the $^{48}\mathrm{Ti}(p,p'\gamma)^{48}\mathrm{Ti}$ reaction with resonance excitation in the compound nucleus $^{49}\mathrm{V}$. The linear correlation coefficients for the reduced widths and amplitudes in the decay of proton resonances with spin $J^\pi=\frac{3}{2}^+$ in $^{49}\mathrm{V}$ are given in Table VI. The statistical significance of the results is given in %. The data in this table show[138,139] that there are nonstatistical correlations of both the reduced amplitudes γ_i and the reduced widths γ_i^2 for protons in resonance decay via different spin channels in the $^{48}\mathrm{Ti}(p,p'\gamma)^{48}\mathrm{Ti}$ reaction. Similar results have also been obtained for a number of other nuclei (Refs. 4, 10, 134, 138, and 139).

An example of the distribution of the amplitude ratios δ_s for proton inelastic scattering in different spin channels via resonances of the compound nucleus $^{49}\mathrm{V}$ in the reaction $^{49}\mathrm{Ti}(p,p'\gamma)^{49}\mathrm{Ti}$ is given in Fig. 23 (Refs. 138 and 139). In this figure the dashed line shows the results calculated in the statistical model, which differ significantly from the experimental data. Therefore, nonstatistical effects are clearly seen in proton inelastic scattering via resonances of a compound nucleus.

Meanwhile, the resonances excited in reactions involving neutrons are, as a rule, poorly described by the statistical model.[140] This great difference between the properties of neutron and proton resonances can be attributed to the presence of a neutron excess. In fact, by bombarding a nucleus with $N-Z>0$ with protons, it is possible to excite very simple configurations of the type $[\pi p\otimes\nu h]_{1^+}$. The cross section for exciting these configurations in the energy range in question is sizable only when there is a neutron excess in the nucleus, i.e., for $N-Z>0$. On the other hand, nonstatistical effects indicate the present of a certain symmetry of the nuclear interaction. Nonstatistical effects due to $[\pi p\otimes\nu h]_{1^+}$ configurations are associated with the spin–isospin $SU(4)$ symmetry of the nuclear interaction, and $SU(4)$ symmetry effects can be enhanced as the neutron excess grows.[79] In $^{58,60,62}\mathrm{Ni}(p,\gamma)^{59,61,63}\mathrm{Cu}$ reactions, nonstatistical effects are

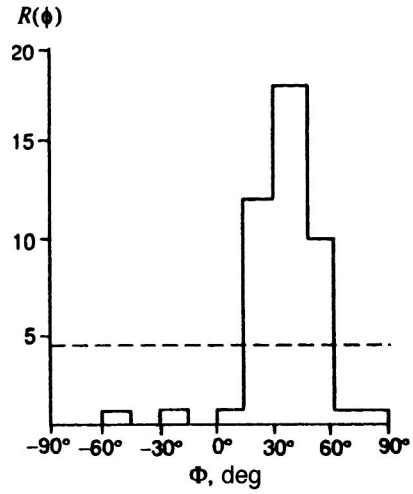

FIG. 23. Distribution of experimental values of $\Phi = \arctan(\gamma_{25}/\gamma_{05})$ for $\frac{3}{2}^-$ resonances in ^{49}V. The statistical model must always give a distribution symmetric about $\Phi = 0$. The distribution of experimental values of Φ is clearly asymmetric about $\Phi = 0$. The dashed line shows the results of the calculation in the statistical model for $\langle \gamma_{25}^2/\gamma_{05}^2 \rangle = 1$, where $\langle \gamma_{ij}^2 \rangle$ is the average value of the reduced width for the corresponding spin channel.

associated with excitation of the $[\pi p \otimes \nu h]_{1^+}$ and $\{[\pi p_I \otimes \nu h_J]_{1^+} \otimes \nu p_J\}_{3/2}$ components in the resonance wave functions.[9,131] Therefore, analysis of the γ decay of nonanalog resonances in ^{58,60,62}Ni$(p,\gamma)^{59,61,63}$Cu reactions indicates the presence of a partial $SU(4)$ symmetry of the nuclear interaction. Since nonstatistical effects are less clearly expressed for nonanalog resonances than for analog resonances,[6,12,132] the $SU(4)$ spin–isospin symmetry is, as expected, a more approximate symmetry than the isospin symmetry of the nuclear interaction.

CONCLUSION

In this review we have presented the results of studies of a number of nonstatistical effects in nuclear decays and nuclear reactions occurring with compound-nucleus formation.

The analysis of the complete set of experimental and theoretical results presented in this review unambiguously shows that nonstatistical effects associated with elementary nuclear excitation modes are present in nuclei. Only when nonstatistical effects are taken into account is it possible to correctly describe a large number of processes occurring in nuclei and nuclear reactions. It is expected that nonstatistical effects will be more strongly manifested in nuclei very far from the stability band.

[1] A. Bohr and B. R. Mottelson, *Nuclear Structure*, Vol. 1 (Benjamin, New York, 1969) [Russ. transl., Mir, Moscow, 1971].
[2] P. G. Hansen, Adv. Nucl. Phys. **7**, 159 (1973).
[3] A. M. Lane, Ann. Phys. (N.Y.) **63**, 171 (1971).
[4] W. K. Wells, E. G. Bilpuch, and G. E. Mitchell, Z. Phys. A **297**, 215 (1980).
[5] Yu. V. Naumov, A. A. Bykov, and I. N. Izosimov, Fiz. Élem. Chastits At. Yadra **14**, 420 (1983) [Sov. J. Part. Nucl. **14**, 175 (1983)].
[6] Yu. V. Naumov and O. E. Kraft, *Isospin in Nuclear Physics* [in Russian] (Nauka, Leningrad, 1971).
[7] J. P. Elliott and P. G. Dawber, *Symmetry in Physics*, Vol. 1 (Macmillan, London, 1979) [Russ. transl., Mir, Moscow, 1983].
[8] Yu. V. Gaponov and Yu. S. Lyutostanskiĭ, Yad. Fiz. **19**, 62 (1974) [Sov. J. Nucl. Phys. **19**, 33 (1974)].
[9] I. N. Izosimov, in *Proceedings of the Intern. School-Seminar on Heavy Ion Physics* [in Russian], edited by Yu. Ts. Oganessian, Yu. E. Penionzhkevich, and R. Kalpakchieva, Dubna, 1993, p. 528.
[10] J. F. Shriner, Jr., E. G. Bilpuch, C. R. Westerfeldt, and G. E. Mitchell, Z. Phys. A **305**, 307 (1982).
[11] O. E. Kraft, Yu. V. Naumov, V. M. Sigalov, and I. V. Sizov, Fiz. Élem. Chastits At. Yadra **17**, 1283 (1986) [Sov. J. Part. Nucl. **17**, 573 (1986)].
[12] I. N. Izosimov, S. S. Parzhitskiĭ, and I. V. Sizov, Izv. Akad. Nauk SSSR, Ser. Fiz. **52**, 78 (1988) [Bull. Acad. Sci. USSR, Phys. Ser.].
[13] I. N. Izosimov, O. E. Kraft, S. S. Parzhitskiĭ *et al.*, Izv. Akad. Nauk SSSR, Ser. Fiz. **52**, 72 (1988) [Bull. Acad. Sci. USSR, Phys. Ser.].
[14] I. N. Izosimov and Yu. V. Naumov, Izv. Akad. Nauk SSSR, Ser. Fiz. **42**, 2248 (1978) [Bull. Acad. Sci. USSR, Phys. Ser.].
[15] I. N. Izosimov, Izv. Akad. Nauk SSSR, Ser. Fiz. **53**, 2451 (1989) [Bull. Acad. Sci. USSR, Phys. Ser.].
[16] B. S. Dzhelepov, L. N. Zyryanova, and Yu. P. Suslov, *Beta Processes* [in Russian] (Nauka, Leningrad, 1972), p. 51.
[17] J. Fujita and K. Ikeda, Nucl. Phys. **67**, 145 (1965).
[18] K. Ikeda, Prog. Theor. Phys. **31**, 434 (1964).
[19] P. M. Endt, in *Nuclear Structure*, edited by A. Hossain (North-Holland, Amsterdam, 1967).
[20] C. Gaarde, K. Kemp, Yu. V. Naumov, and P. R. Amundsen, Nucl. Phys. A **143**, 497 (1970).
[21] Yu. V. Naumov and O. E. Kraft, Fiz. Élem. Chastits At. Yadra **6**, 892 (1975) [Sov. J. Part. Nucl. **6**, 361 (1975)].
[22] R. R. Doering, A. Galonsky, D. M. Patterson, and G. Bertsch, Phys. Rev. Lett. **35**, 1691 (1975).
[23] D. J. Horen, C. D. Goodman, D. E. Bainum *et al.*, Phys. Lett. B **99**, 383 (1981).
[24] Yu. V. Naumov, I. N. Izosimov, B. F. Petrov, and A. A. Bykov, Report D7-80-556, JINR, Dubna (1980), p. 55 [in Russian].
[25] A. A. Bykov, I. N. Izosimov, Yu. V. Naumov, and B. F. Petrov, in *Abstracts of the Thirty-First Meeting on Nuclear Spectroscopy and Nuclear Structure* [in Russian] (Nauka, Leningrad, 1981), p. 333.
[26] K.-L. Kratz, W. Rudolph, H. Ohm *et al.*, *Investigation of Beta Strength Functions by Neutron and Gamma Ray Spectroscopy* (Institut für Kernchemie, Mainz, 1978).
[27] A. A. Bykov, V. D. Vitman, Yu. V. Naumov *et al.*, Preprint No. 628, Leningrad Nuclear Physics Institute, Leningrad (1980) [in Russian]; Izv. Akad. Nauk SSSR, Ser. Fiz. **45**, 874 (1981) [Bull. Acad. Sci. USSR, Phys. Ser.].
[28] I. N. Izosimov, V. G. Kalinnikov, M. Yu. Myakushin *et al.*, Preprint E6-96-454, JINR, Dubna (1996) [in Russian]; J. Phys. G **24**, 831 (1998).
[29] A. Bohr and B. R. Mottelson, *Nuclear Structure*, Vol. 2 (Benjamin, New York, 1975) [Russ. transl., Mir, Moscow, 1977].
[30] Yu. V. Naumov and O. E. Kraft, in *Proceedings of the Eleventh Winter School of the Leningrad Nuclear Physics Institute on Nuclear and Elementary Particle Physics* [in Russian] (Leningrad Nuclear Physics Institute, Leningrad, 1976), p. 34.
[31] H. V. Klapdor, C. O. Wene, I. N. Izosimov, and Yu. V. Naumov, Phys. Lett. B **78**, 20 (1978).
[32] H. V. Klapdor, C. O. Wene, I. N. Izosimov, and Yu. V. Naumov, Z. Phys. A **292**, 249 (1979).
[33] I. N. Borzov, E. L. Trykov, and S. A. Fayans, in *Proceedings of the Twenty-Fourth Winter School of the Leningrad Nuclear Physics Institute on Nuclear and Elementary Particle Physics* [in Russian] (Leningrad Nuclear Physics Institute, Leningrad, 1989), p. 331.
[34] V. G. Guba, M. A. Nikolaev, and M. G. Urin, in *Proceedings of the Twenty-Fourth Winter School of the Leningrad Nuclear Physics Institute on Nuclear and Elementary Particle Physics* [in Russian] (Leningrad Nuclear Physics Institute, Leningrad, 1989), p. 364.
[35] K. Takahashi, M. Yamada, and T. Kondon, At. Data Nucl. Data Tables **12**, 101 (1973).
[36] K. Takahashi and M. Yamada, Prog. Theor. Phys. **41**, 1470 (1969).
[37] Yu. V. Gaponov and Yu. S. Lyutostanskiĭ, *Isobar States of Spherical Nuclei* [in Russian] (IAE, Moscow, 1974).
[38] Yu. V. Gaponov and Yu. S. Lyutostanskiĭ, Fiz. Élem. Chastits At. Yadra **12**, 1324 (1981) [Sov. J. Part. Nucl. **12**, 528 (1981)].
[39] P. Möller and J. Randrup, Nucl. Phys. A **514**, 1 (1990).
[40] A. Staudt, E. Bender, K. Muto, and H. V. Klapdor-Kleingrothaus, At. Data Nucl. Data Tables **44**, 79 (1990).

[41] G. J. Mathews, S. D. Bloom, G. M. Fuller, and J. N. Bahcall, Phys. Rev. C **32**, 796 (1985).
[42] J. Krumlinde and P. Möller, Nucl. Phys. A **417**, 420 (1984).
[43] T. Izumoto, Nucl. Phys. A **395**, 189 (1983).
[44] N. I. Pyatov and S. A. Fayans, Fiz. Élem. Chastits At. Yadra **14**, 953 (1983) [Sov. J. Part. Nucl. **14**, 401 (1983)].
[45] I. N. Borzov and S. A. Fayans, Preprint No. 1129, FÉI (1981) [in Russian].
[46] V. G. Solov'ev, *Theory of the Nucleus. Quasiparticles and Phonons* (Institute of Physics, Bristol, 1992) [Russ. original, Énergoatomizdat, Moscow, 1989].
[47] V. A. Kuzmin and V. G. Soloviev, J. Phys. G **10**, 1507 (1984).
[48] S. E. Murav'ev and M. G. Urin, Izv. Akad. Nauk SSSR, Ser. Fiz. **53**, 973 (1989) [Bull. Acad. Sci. USSR, Phys. Ser.].
[49] I. N. Izosimov, S. G. Yavshits, and S. A. Egorov, in *Proceedings of the Intern. School-Seminar on Heavy Ion Physics* [in Russian], Dubna, 1989, D7-90-142, p. 287.
[50] F. Frisk, I. Hamamoto, and X. Z. Zang, Preprint Lund-Mph-95/09, Lund (1995); Phys. Rev. C **52**, 2468 (1996).
[51] E. Bender, K. Muto, and H. V. Klapdor, Phys. Lett. B **208**, 53 (1988).
[52] P. Möller and J. Randrup, Preprint LBL-27504, Berkeley (1989); Nucl. Phys. A **514**, 1 (1990).
[53] M. A. Preston, *Physics of Nuclei* (Addison-Wesley, Reading, Mass., 1962).
[54] N. B. Gove and M. J. Martin, Nucl. Data Tables **10**, 205 (1971).
[55] A. A. Bykov, V. D. Vitman, Yu. V. Naumov *et al.*, Preprint No. 647, Leningrad Nuclear Physics Institute, Leningrad, 1981; Izv. Akad. Nauk SSSR, Ser. Fiz. **46**, 2230 (1982) [Bull. Acad. Sci. USSR, Phys. Ser.].
[56] B. Jonson, E. Hagberg, P. G. Hansen *et al.*, in *Proceedings of the Conf. on Nuclei Far from Stability*, Cargèse, France, 1976, CERN Report 76-13, p. 277.
[57] A. A. Bykov, V. D. Vitman, V. F. Moroz, and Yu. V. Naumov, Izv. Akad. Nauk SSSR, Ser. Fiz. **44**, 918 (1980) [Bull. Acad. Sci. USSR, Phys. Ser.].
[58] V. A. Karnaukhov and L. A. Petrov, *Nuclei Far from the β Stability Band* [in Russian] (Énergoatomizdat, Moscow, 1981).
[59] K.-L. Kratz, H. Ohm, K. Summerer *et al.*, Phys. Lett. B **86**, 21 (1979).
[60] Yu. V. Naumov, O. E. Kraft, B. F. Petrov *et al.*, Fiz. Élem. Chastits At. Yadra **9**, 1282 (1978) [Sov. J. Part. Nucl. **9**, 502 (1978)].
[61] P. G. Hansen and B. Jonson, in *Charged Particle Emission from Nuclei*, edited by D. N. Poenaru and M. S. Ivascu (CRC, Boca Raton, 1989), p. 21.
[62] *Table of Radioactive Isotopes*, edited by E. Browne and R. B. Firestone (New York, 1986); *Table of Isotopes*, edited by G. M. Lederer and J. S. Shirly (New York, 1978).
[63] J. C. Hardy, Report 76-13, CERN, Geneva (1976), p. 267.
[64] D. D. Bogdanov, V. A. Karnaukhov, and L. A. Petrov, Yad. Fiz. **18**, 3 (1973) [Sov. J. Nucl. Phys. **18**, 1 (1974)].
[65] K.-L. Kratz, J. Krumlinde, G. A. Leander, and P. Möller, ACS Symp. Ser. **324**, 159 (1986).
[66] T. Jahnsen, A. C. Pappas, and T. Tunaal, *Delayed Fission Neutrons* (IAEA, Vienna, 1968).
[67] K.-L. Kratz, A. Ohm, A. Schroder *et al.*, in *Proceedings of the Intern. Conf. on Nuclei Far from Stability*, Helsinger, 1981, p. 317.
[68] H. V. Klapdor, J. Metzinger, T. Oda *et al.*, Preprint MPI H, Vol. 24 (1981).
[69] Y. Nir-El and S. Amiel, Report 76-13, CERN, Geneva (1976).
[70] I. C. Hardy, L. C. Carraz, B. Jonson, and G. Hansen, Phys. Lett. B **71**, 307 (1971).
[71] I. N. Izosimov, in *Proceedings of the Intern. Conf. on Exotic Nuclei*, edited by Yu. E. Penionzhkevich, R. Kalpakchieva, and R. Foros, Crimea, 1991, p. 214.
[72] R. C. Greenwood, R. G. Helmer, M. H. Putnam, and K. D. Watts, Nucl. Instrum. Methods Phys. Res. A **390**, 95 (1997).
[73] M. Karny, J. M. Nitschke, L. F. Archambault *et al.*, Preprint 96-63, GSI, Darmstadt (1996).
[74] A. A. Bykov, V. D. Vitman, Yu. V. Naumov *et al.*, Preprint No. 748, Leningrad Nuclear Physics Institute, Leningrad (1982) [in Russian].
[75] V. G. Kalinnikov, K. Ya. Gromov, M. Yanicki *et al.*, Nucl. Instrum. Methods Phys. Res. B **70**, 62 (1992).
[76] J. Wawryszczuk, M. B. Yuldashev, K. Ya. Gromov *et al.*, Z. Phys. A **357**, 39 (1997).
[77] I. N. Izosimov, in *Proceedings of the Intern. Conf. on Nuclear Data for Science and Technology*, Trieste, Italy, 1997, p. 91.
[78] H. V. Klapdor, J. Metzinger, and T. Oda, At. Data Nucl. Data Tables **31**, 81 (1984).
[79] I. N. Izosimov, Preprint E7-93-126, JINR, Dubna (1993), p. 74.
[80] É. E. Berlovich and Yu. N. Novikov, Dokl. Akad. Nauk SSSR **185**, 1025 (1969) [Sov. Phys. Dokl. **14**, 349 (1969)].
[81] V. M. Kuznetsov, N. K. Skobelev, and G. N. Flerov, Yad. Fiz. **4**, 279 (1966) [Sov. J. Nucl. Phys. **4**, 202 (1967)].
[82] N. K. Skobelev, Yad. Fiz. **15**, 444 (1972) [Sov. J. Nucl. Phys. **15**, 249 (1972)].
[83] V. I. Kuznetsov, Fiz. Élem. Chastits At. Yadra **12**, 1285 (1981) [Sov. J. Part. Nucl. **12**, 511 (1981)].
[84] L. G. Belov, Yu. P. Gangrskiĭ, M. B. Miller *et al.*, Preprint R15-9795, JINR, Dubna (1976) [in Russian].
[85] Yu. P. Gangrskiĭ, G. M. Marinescu, M. B. Miller *et al.*, Preprint R15-10613, JINR, Dubna (1977) [in Russian]; Yad. Fiz. **27**, 894 (1978) [Sov. J. Nucl. Phys. **27**, 475 (1978)].
[86] L. Kh. Batist, É. E. Berlovich, V. V. Gavrilov *et al.*, Preprint No. 363, Leningrad Nuclear Physics Institute, Leningrad (1977) [in Russian].
[87] V. I. Kuznetsov, N. K. Skobelev, and G. N. Flerov, Yad. Fiz. **5**, 271 (1967) [Sov. J. Nucl. Phys. **5**, 191 (1967)].
[88] D. Habs, H. Kleve-Nebenius, V. Metag *et al.*, Z. Phys. A **285**, 53 (1978).
[89] Yu. P. Gangrskiĭ, M. B. Miller, I. F. Kharisov *et al.*, Preprint R7-10797, JINR, Dubna (1977) [in Russian]; Yad. Fiz. **31**, 306 (1980) [Sov. J. Nucl. Phys. **31**, 162 (1980)].
[90] H. L. Hall, K. E. Gregorich, R. A. Henderson *et al.*, Phys. Rev. C **39**, 1866 (1989).
[91] H. L. Hall, K. E. Gregorich, R. A. Henderson *et al.*, Phys. Rev. C **41**, 618 (1990).
[92] Yu. A. Lazarev, Yu. Ts. Oganessian, I. V. Shirokovsky *et al.*, Europhys. Lett. **4**, 893 (1987).
[93] Yu. A. Lazarev, Yu. Ts. Oganessian, I. V. Shirokovsky *et al.*, in *Proceedings of the Intern. Conf. on Fifty Years Research in Nuclear Fission*, Berlin, 1989, p. 6.
[94] S. M. Polikanov, *Nuclear Shape Isomerism* [in Russian] (Atomizdat, Moscow, 1977).
[95] H. V. Klapdor-Kleingrothaus, in *Proceedings of the Intern. School–Seminar on Heavy Ion Physics* [in Russian], Dubna, 1990, D7-90-142, JINR, Dubna, p. 440.
[96] P. Axel, Phys. Rev. **126**, 671 (1962).
[97] V. A. Ageev, V. Ya. Golovnya, E. A. Gromova *et al.*, Yad. Fiz. **46**, 700 (1987) [Sov. J. Nucl. Phys. **46**, 392 (1987)].
[98] V. M. Strutinsky, Nucl. Phys. A **95**, 420 (1967).
[99] P. Möller and J. R. Nix, in *Proceedings of the Third IAEA Symp. on Physics and Chemistry of Fission*, Rochester, NY, 1973 (IAEA, Vienna, 1974), Vol. 1, p. 103.
[100] S. P. Ivanova, A. L. Komov, L. A. Malov, and V. G. Solov'ev, Fiz. Élem. Chastits At. Yadra **7**, 450 (1976) [Sov. J. Part. Nucl. **7**, 175 (1976)].
[101] A. H. Wapstra and K. A. Bos, At. Data Nucl. Data Tables **17**, 274 (1976).
[102] K.-L. Kratz, W. Rudolph, H. Ohm *et al.*, Nucl. Phys. A **317**, 335 (1979).
[103] K.-L. Kratz, W. Rudolph, H. Ohm *et al.*, Phys. Lett. B **65**, 231 (1976).
[104] Yu. Ts. Oganessian and Yu. A. Lazarev, in *Treatise on Heavy Ion Science*, edited by D. A. Bromley (Plenum, New York, 1985), Vol. 4, p. 3.
[105] Yu. A. Lazarev, Yu. Ts. Oganesyan, S. P. Tret'yakova *et al.*, in *Proceedings of the Intern. School–Seminar on Heavy Ion Physics* [in Russian], Dubna, 1990, D7-90-142, JINR, Dubna, p. 208.
[106] K. A. Mezilev, Yu. N. Novikov, A. V. Popov *et al.*, in *Proceedings of the Intern. School–Seminar on Heavy Ion Physics* [in Russian], Dubna, 1990, D7-90-142, JINR, Dubna, p. 199.
[107] I. N. Izosimov, Izv. Ross. Akad. Nauk, Ser. Fiz. **57**, 29 (1993) [Bull. Russ. Acad. Sci., Phys. Ser.].
[108] P. Möller and J. R. Nix, At. Data Nucl. Data Tables **26**, 165 (1981).
[109] H. V. Klapdor, Fortschr. Phys. **33**, 1 (1985).
[110] I. N. Izosimov, Izv. Akad. Nauk SSSR, Ser. Fiz. **56**, 39 (1992) [Bull. Acad. Sci. USSR, Phys. Ser.].
[111] F.-K. Thielemann, J. Metzinger, and H. V. Klapdor, Z. Phys. A **309**, 310 (1983).
[112] V. V. Pashkevich, in *Proceedings of the Intern. School–Seminar on Heavy Ion Physics*, Alushta, USSR, 1983, D7-83-644, JINR, Dubna (1983), p. 405.
[113] S. A. Egorov, V. A. Rubchenya, and S. V. Khlebnikov, Yad. Fiz. **46**, 60 (1987) [Sov. J. Nucl. Phys. **46**, 38 (1987)].
[114] J. Weber, H. C. Britt, A. Gavron *et al.*, Phys. Rev. C **13**, 2413 (1976).
[115] F.-K. Thelemann and M. Wiescher, in *Primordial Nucleosynthesis*, edited

by W. Thompson and B. Carney (World Scientific, Singapore, 1990), p. 92.
[116] D. Morrisey, in *Unstable Nuclei in Astrophysics*, edited by S. Kubono and T. Kajino (World Scientific, Singapore, 1991), p. 12.
[117] M. Hashimoto, K. Nomoto, and T. Shigeyama, Astron. Astrophys. **210**, L5 (1989).
[118] A. G. W. Cameron, in *Cosmic Abundances of Matter*, edited by C. J. Waddington, AIP Conf. Proc., Vol. 183 (1989), p. 349.
[119] Ya. M. Kramarovskiĭ and V. P. Chechev, *Element Synthesis in the Universe* [in Russian] (Nauka, Moscow, 1987).
[120] E. M. Burbidge, G. R. Burbidge, W. A. Fowler, and F. Hoyle, Rev. Mod. Phys. **29**, 547 (1957).
[121] F.-K. Thielemann and K.-L. Kratz, Preprint IKMz 91-4, Universität Mainz (1991).
[122] C. O. Wene, Astron. Astrophys. **44**, 233 (1975).
[123] D. N. Schramm and G. S. Wasserbyrg, Astrophys. J. **162**, 57 (1970).
[124] H. V. Klapdor and C. O. Wene, Astrophys. J. Lett. **230L**, 113 (1979).
[125] I. N. Izosimov and Yu. V. Naumov, in *Abstracts of the Thirtieth Meeting on Nuclear Spectroscopy and Nuclear Structure* [in Russian] (Nauka, Leningrad, 1980), p. 265.
[126] C. O. Wene and S. A. E. Johansson, Report 76-13, CERN, Geneva (1976), p. 584.
[127] D. N. Schramm, Annu. Rev. Astron. Astrophys. **12**, 383 (1974).
[128] W. A. Fowler, Colorado Associated Univ. Press, 1972, p. 66; Proc. R. A. Welch Foundation Conf. on Chem. Rev. XXI Cosmochemistry, Houston, 1978, p. 61.
[129] Yu. V. Naumov, Izv. Akad. Nauk SSSR, Ser. Fiz. **39**, 1645 (1975) [Bull. Acad. Sci. USSR, Phys. Ser.].
[130] I. N. Izosimov, O. E. Kraft, S. S. Parzhitskiĭ, and I. V. Sizov, Report R15-87-256, JINR, Dubna (1987) [in Russian].
[131] I. N. Izosimov, in *Proceedings of the Eighth Intern. Symp. on Capture Gamma-Ray Spectroscopy*, edited by J. Kern, Switzerland, 1983, p. 593.
[132] I. N. Izosimov, O. E. Kraft, Yu. V. Naumov, and V. M. Sigalov, Izv. Akad. Nauk SSSR, Ser. Fiz. **50**, 1952 (1986) [Bull. Acad. Sci. USSR, Phys. Ser.].
[133] O. E. Kraft, Yu. V. Naumov, S. S. Parzhitskiĭ, and I. V. Sizov, Izv. Akad. Nauk SSSR, Ser. Fiz. **40**, 1182 (1976) [Bull. Acad. Sci. USSR, Phys. Ser.].
[134] G. E. Mitchell, T. R. Dittrich, and E. G. Bilpuch, Z. Phys. A **289**, 211 (1979).
[135] I. N. Izosimov, in *Proceedings of the European Physical Society Fifteenth Nuclear Physics Divisional Conf.*, St. Petersburg, Russia, 1995, p. 635.
[136] V. E. Bunakov, in *Proceedings of the Seventh Winter School of the Leningrad Nuclear Physics Institute on Nuclear and Elementary Particle Physics* [in Russian] (Leningrad Nuclear Physics Institute, Leningrad, 1972), p. 46.
[137] M. G. Kendall and A. Stuart, *The Advanced Theory of Statistics*, 4th ed. (Griffin, London, 1977) [Russ. transl. of earlier ed., Nauka, Moscow, 1966].
[138] B. H. Chou, G. E. Mitchell, E. G. Bilpuch, and C. R. Westerfeldt, Z. Phys. A **300**, 157 (1981).
[139] P. Ramakrishnan, B. H. Chou, G. E. Mitchell *et al.*, Z. Phys. A **311**, 160 (1983).
[140] F. Bechvarzh, Ya. Gonzatko, M. Kralik *et al.*, Report R3-12516, JINR, Dubna (1979) [in Russian].

Translated by Patricia A. Millard